# Cytosolic glucosylceramide regulates endolysosomal function in Niemann-Pick type C disease

**Preprint** · March 2019

CITATIONS
0

READS
158

**10 authors**, including:

Simon Wheeler
De Montfort University
**19** PUBLICATIONS **87** CITATIONS
SEE PROFILE

Meenakshi Bhardwaj
De Montfort University
**1** PUBLICATION **0** CITATIONS
SEE PROFILE

Maria Joao Ferraz
Leiden University
**43** PUBLICATIONS **673** CITATIONS
SEE PROFILE

Hein Sprong
National Institute for Public Health and the Environment (RIVM)
**290** PUBLICATIONS **7,753** CITATIONS
SEE PROFILE

# Cytosolic glucosylceramide regulates endolysosomal function in Niemann-Pick type C disease

Simon Wheeler[1], Per Haberkant[2], Meenakshi Bhardwaj[1], Paige Tongue[1], Maria J. Ferraz[4], David Halter[3], Hein Sprong[6] , Ralf Schmid[5], Johannes M. F. G. Aerts[4], Nikol Sullo[1], Dan J. Sillence*[1]

Highlights:

A new paradigm for Niemann-Pick C disease is presented where lysosomal storage leads to a deficit in cytoplasmic glucosylceramide (GlcCer) where it performs important functions.

Previously it had been reported that Gaucher cells have defective endolysosomal pH. GlcCer also accumulates in Niemann-Pick C disease and also shows this defect.

Niemann-Pick C cells were found to have reduced cytoplasmic glucosylceramide (GlcCer) transport.

Inhibiting cytoplasmic glucocerebrosidase (GBA2), increased GlcCer, decreased endolysosomal pH in normal cells, reversed increases in endolysosomal pH and restored disrupted BODIPY-LacCer trafficking and increased expression of vATPase a subunit in Niemann-Pick C fibroblasts.

The results are consistent with a model where both endolysosomal pH and Golgi targeting of BODIPY-LacCer are dependent on adequate levels of cytosolic GlcCer which are reduced in NPC disease.

This work consequently suggests GBA2 and vATPase as new therapeutic targets in Niemann-Pick C and related neurodegenerative diseases.

# Cytosolic glucosylceramide regulates endolysosomal function in Niemann-Pick type C disease

Simon Wheeler[1], Per Haberkant[2], Meenakshi Bhardwaj[1], Paige Tongue[1], Maria J. Ferraz[4], David Halter[3], Hein Sprong[6] , Ralf Schmid[5], Johannes M. F. G. Aerts[4], Nikol Sullo[1], Dan J. Sillence*[1]

From the [1]School of Pharmacy, De Montfort University, The Gateway, Leicester, LE1 9BH, UK; [2]European Molecular Biology Laboratory, Myerhofstraße 1, 69117, Heidelberg, Germany; [3]Philips Research Eindhoven, High Tech Campus 34, 5656 AE Eindhoven, The Netherlands; [4]Leiden Institute of Chemistry, Leiden University, 2300 RA, Leiden, The Netherlands; [5]Department of Molecular and Cell Biology, Henry Wellcome Building, University of Leicester, Lancaster Road, Leicester, LE1 7RH, UK; [6]National Institute of Public Health and Environment, Laboratory for Zoonoses and Environmental Microbiology, Antonie van Leeuwenhoeklaan 9, P.O. Box 13720 BA Bilthoven, The Netherlands

Running title: Glucosylceramide acidifies NPC lysosomes

**Keywords**: sphingolipid; glycolipids; endocytosis; neurodegenerative disease; lysosomal acidification

*To whom correspondence should be addressed: Dan J Sillence, School of Pharmacy, De Montfort University, The Gateway, Leicester, LE1 9BH, UK; dsillence@dmu.ac.uk; (44) 116 2506368

**Abstract**

Niemann-Pick type C disease (NPCD) is a neurodegenerative disease associated with increases in cellular cholesterol and glycolipids and most commonly caused by defective NPC1, a late endosomal protein. Using ratiometric probes we find that NPCD cells show increased endolysosomal pH. In addition U18666A, an inhibitor of NPC1, was found to increase endolysosomal pH, and the number, size and heterogeneity of endolysosomal vesicles. NPCD fibroblasts and cells treated with U18666A also show disrupted targeting of fluorescent lipid BODIPY-LacCer to high pH vesicles. Inhibiting non-lysosomal glucocerebrosidase (GBA2) reversed increases in endolysosomal pH and restored disrupted BODIPY-LacCer trafficking in NPCD fibroblasts. GBA2 KO cells also show decreased endolysosomal pH. NPCD fibroblasts also show increased expression of a key subunit of the lysosomal proton pump vATPase on GBA2 inhibition. The results are consistent with a model where both endolysosomal pH and Golgi targeting of BODIPY-LacCer are dependent on adequate levels of cytosolic-facing GlcCer, which are reduced in NPC disease.

Niemann-Pick type C disease (NPCD) is a devastating neurodegenerative condition most commonly due to mutations in NPC1 [1,2] a protein of late endosomes and lysosomes [3]. (Due to difficulties in precisely distinguishing these two sets of organelles the term endolysosome will be used here to include both.) Mutations in NPC1 are associated with impaired endocytic transport via decreased endolysosomal calcium release [4,5]. In turn, endocytosis and luminal calcium are dependent on correct endolysosomal acidification [4] and have been found to be controlled by glycolipids in neurons [6], melanocytes [7], plant vacuoles [8] and *C. elegans* [9]. It is increasingly apparent that aberrant lysosomal GlcCer in Gaucher disease is associated with elevated endolysosomal pH [10–13]. Glycolipids, vital for mammals [14], are also implicated in membrane trafficking [10,15]. Similarly in yeast the NPC1 homologue ncr1 regulates both vacuolar pH [16] and glycolipid transport [17]. An overview of sphingolipid metabolism highlighting the connection with endocytosis is offered in Fig. S1.

Does NPC1 affect endolysosomal pH? Conflicting evidence has been found both in disease fibroblasts [5,16,18–20] and in cells treated with U18666A, a putative inhibitor of NPC1 [5,21–23]. If endocytic traffic is delayed then probes which permeate all acidic organelles will show increased pH values even though fully mature lysosomes still acidify correctly. We used such a general probe to measure endolysosomal pH in NPCD cells and cells treated with U18666A

and found the pH higher than normal. Endocytosis was also disrupted.

To address these issues we also examined glycolipid transport. NPCD cells and culture models were found to have decreased non-vesicular glucosylceramide (GlcCer) transport. In contrast, inhibiting non-lysosomal glucocerebrosidase (GBA2) decreased endolysosomal pH in normal cells, reversed increases in endolysosomal pH, increased ATP6V0a1 expression and restored disrupted BODIPY-LacCer trafficking in NPCD fibroblasts. The results are consistent with a model where both endolysosomal pH and Golgi targeting of BODIPY-LacCer are dependent on adequate levels of GlcCer on the cytosolic face of membranes; NPC disease reduces this lipid subpopulation.

## Results

### *U18666A increases the size and pH of the endolysosomal compartment*

An NPC disease phenotype can be induced by a variety of cationic amphiphiles (which also inhibit filoviral fusion) [23–25]. Previously it has been reported that the cationic amphiphile U18666A increases the pH of endolysosomes as measured by fluorescence ratio imaging [21]. Since acidification is a critical step in endosomal maturation the endolysosomal pH of U18666A-treated RAW macrophages was measured using acridine orange as a pH sensor. Acridine orange accumulates within endolysosomes due to protonation and changes colour from green to red. Fig. 1A,D show that U18666A treatment decreases the red/green ratio of punctates labelled with acridine orange (control 2.2 ± 0.2 to 1.0±0.1 U18666A treated), consistent with an alkalinising effect on endolysosomes. U18666A treatment also increased the size (Fig. 1E) and red/green heterogeneity (Fig. 1A) of acridine labelled punctates, similar to what has been reported before [26–28]. In order to control for changes in lysosome size experiments were performed with $NH_4Cl$ which led to similar decreases in red/green ratio alone or in the presence of U18666A (Fig. 1D).

### *Niemann-Pick C cells show increased endolysosomal pH*

Due to potential pitfalls of acridine orange staining such as unequal loading and effects of cholesterol [29] further experiments were performed using LysoSensor yellow/blue [30] as a ratiometric probe which changes colour in a concentration-independent manner. Using this probe we obtained a pH value for the total endolysosomal compartment of RAW cells of 5.4±0.1; treatment with 5 μM U18666A for 2.25 hours increased this to 6.4±0.3 (Fig. 2A,B).
Control fibroblasts gave a value of 4.5±0.1 in line with previously reported values [31,32] while in NPC patient fibroblasts this increased to 5.4±0.3; patient lymphoblasts showed similar increases in total endolysosomal pH (Fig. 2A). (For correlation curves see Fig. S2.) This increase in NPCD endolysosomal pH is in agreement with previous studies [19,20] and with reports that GlcCer accumulation leads to delayed endolysosomal acidification [19–21]. It is not inconsistent with contrary observations of mature NPCD lysosomes – this issue will be addressed again in the discussion section.

We were also interested in the kinetics of pH increase resulting from U18666A treatment. In RAW cells endolysosomal pH increased over three hours on U18666A treatment (Fig. 2B), though the rise was evident after 45 minutes and mostly complete by 2 hours. Thus the pH increase with this agent precedes the accumulation of both cholesterol [5] and GlcCer (Fig. 6D).

### *BODIPY-LacCer traffics to a high pH compartment in U18666A-treated RAW macrophages and NPC fibroblasts*

BODIPY-LacCer can be used as a marker of endocytosis. This fluorescent lipid traffics from late endosomes to the Golgi via a pathway dependent on NPC1, rab 7/9 and TRPML1 [33,34]; correct endolysosomal acidification is also important for the successful completion of endocytosis [35–38]. In many glycolipid storage diseases such transport is disrupted and instead the fluorescent lipid co-localises with late endosomes and lysosomes [1,39]. Given the effects of U18666A on endolysosomal pH we next studied evidence for BODIPY-LacCer endocytic trafficking to high pH compartments. RAW cells were pulse-labelled with BODIPY-LacCer and, in the presence of U18666A, the fluorescent marker incompletely co-localised with LysoTracker red

(Fig. 3A, Pearson's co-localisation coefficient 0.51±0.01). Further experiments in NPC human fibroblasts were conducted and revealed a similar effect (Fig. 3B, Pearson's co-localisation coefficient 0.17±0.02). This result contrasts with other storage diseases where co-localisation of BODIPY-LacCer and a variety of late endosomal and lysosomal markers [1,39] including LysoTracker red [15] occurs. In NPC cell culture models it appears that BODIPY LacCer sorting is diverted to a high pH compartment (pH > 6.5), consistent with increased endolysosomal pH.

***Inhibition of GBA2 decreases endolysosomal pH and reverses altered BODIPY-LacCer targeting in NPC fibroblasts***

Previous studies have used brefeldin A to merge the ER and Golgi thus co-localising ceramide and GlcCer synthase and increasing the amount of GlcCer on the cytosolic face of membranes ('cytosolic GlcCer') [40]. (In our hands this tactic increased GlcCer levels by about 50% in CHO cells (Fig. 6D), similar findings were obtained in fibroblasts (data not shown).) In fibroblasts, we discovered that endolysosomal pH was lowered under these conditions in both control and disease cells (4.5±0.1 to 4.2±0.1 for control cells, 5.4±0.3 to 4.6±0.1 for NPCD cells, Fig. 4A). The converse is also true: high endolysosomal pH is linked to low levels of GlcCer in melanocytes (7) and mouse macrophages (10). Consequently we increased cytosolic GlcCer by inhibiting its hydrolase GBA2 an enzyme which is upregulated in a mouse model of NPCD [41]. Initial experiments with 6 μM NB-DGJ and 1 μM NB-DNJ lowered endolysosomal pH (data not shown). (Although these imino-sugars have been developed as a GlcCer synthase inhibitors they are more potent GBA2 inhibitors [42]; NB-DNJ (miglustat) is approved for the treatment of NPCD.) We then switched attention to AMP-DNJ [43], a version of NB-DNJ but an even more potent inhibitor of GBA2, which has shown promise in a recent *in vivo* study of a mouse model of NPCD (40). Following precedent [44,45] the use of 20nM AMP-DNJ indeed corrected the endolysosomal pH defect by inhibition of GBA2. Thus the endolysosomal pH of NPC cells reduced from 5.4±0.3 to 4.5±0.17 (Fig. 4B). When normal fibroblasts were subjected to the same treatment the endolysosomal pH also reduced to 4.1±0.08 (Fig. 4B). To exclude the possibility of off-target pharmacology we also measured endolysosomal pH in a near-haploid chronic myelogenous leukaemia cell line (HAP1 cells) Consistent with our previous results, CRISPR genetic knockout of GBA2 led to a decrease in endolysosomal pH (Fig. S3). AMP-DNJ treatment increases total GlcCer between 1-20 nM in NPC fibroblasts (Fig. S4).

Previous experiments in Gaucher disease have suggested that not only endolysosomal pH but also BODIPY-LacCer trafficking are dependent on cytosolic GlcCer levels [15]. Thus inhibiting GlcCer synthase by high concentrations of NB-DNJ and NB-DGJ (100 μM) gave aberrant trafficking which was repaired by specifically replenishing cytosolic GlcCer by adding GlcSph [15]. In order to test if this finding could be replicated in NPCD cells we initially treated NPC fibroblasts with imino-sugars at concentrations where they would be expected to inhibit GBA2 selectively. Fig. 4C,D show reversal of disrupted BODIPY-LacCer targeting using both inhibitors. Representative images from fluorescence microscopy are shown in Fig. 4E-F; BODIPY-TR-ceramide is used as a Golgi marker in these images which therefore show how Golgi targeting can be assessed. Use of NB-DGJ at a concentration expected to inhibit GlcCer synthase (>12μM) did not rectify trafficking (Fig. 4C). The results are consistent with a model where both endolysosomal pH and Golgi targeting of BODIPY-LacCer are dependent on cytosolic GlcCer which is disrupted in NPC disease

***vATPase a subunit expression is increased on GBA2 inhibition***

Our findings above suggest that cytosolic GlcCer is necessary for activation of the endolysosomal proton pump vATPase, as previously argued [7,46]. If this lipid pool is deficient in NPC disease then we may expect altered expression of vATPase subunits. Expression of subunit a (ATP6V0a1) was examined by PCR and western blotting and was equal in both healthy and NPC cells (Fig. 5A-C). In contrast, GBA2 inhibition with AMP-DNJ significantly increased ATP6V0a1 expression at the protein level (Fig. 5A-C) in both cell types. A similar increase was observed with mRNA, though this was not significant. These experiments are consistent with our observations of endolysosomal

pH (Fig. 4A,B). (A dose of 10nM AMP-DNJ had given optimal pH reductions in a variety of other cell types (data not shown) so this concentration was used in the blotting experiments.)

Using the recently determined structure [47] of the yeast homologue (PDB: 5TJ5) as a template we built a model [48,49] of part of the membrane resident portion of human vATPase (3 of the ten c subunits and the a subunit) and validated it using QMEANBrane [50] which indicated acceptable quality (local score 0.50-0.79 for relevant regions, Fig. S5). Using molecular docking software ROSIE [51–53] which allows some flexibility of both sidechains and backbone we found a number of binding poses where the GlcCer headgroup uses hydrogen-bonds to bridge the a and c subunits. An example is shown in Fig. 5D: the headgroup is positioned where the membrane border is expected to be with the tails oriented correctly, (see also the QMEANBrane output in Fig. S5.) This binding is in agreement with a previous report of crosslinking of photoactivatable pacGlcCer with the vATPase c subunit [54].

The vATPase a subunit is highly conserved across eukaryotes. However the predicted critical residue for GlcCer binding only showed a high level of conservation from mammals to GlcCer containing yeast (Fig. 5E). In most non-GlcCer expressing yeast this residue was replaced by a glycine which would not be able to support GlcCer binding (Fig. 5C, S6). This is highly suggestive that this important residue correlates with GlcCer. (The presence of Asp rather than Asn in most GlcCer containing yeasts is not significant as this ionised residue is still able to perform the H-bond acceptor function [55] of Asn depicted in Fig. 5D.)

### *The impact of NPC1 inhibition on transport of GlcCer to the cell surface*

To probe further this putative insufficiency in cytosolic GlcCer we measured cell surface transport which would be likely reduced in NPCD. To this end glycolipid transfer protein (GLTP) was used to extract radiolabelled GlcCer from the cell surface following a previous procedure [56]. GlcCer is transported by both vesicular and non-vesicular mechanisms [56–58] and cytosolic GlcCer levels are limited by translocation (‘flipping’) in the ER and a post-Golgi compartment [56]. Over two hours inhibition of vesicular transport by brefeldin A (BFA) partially inhibited transport of GlcCer to the cell surface by 30-40% while U18666A inhibited GlcCer transport by ~60% even in the presence of BFA (Fig. 6A). Thus U18666A rapidly inhibits non-vesicular GlcCer transport. Broadly similar observations were made in NPC fibroblasts (Fig. 6C). However, inhibition of GlcCer transport did not result in significant increases in GlcCer synthesis and only small increases in levels of this lipid occurred in the timeframe of the experiment (Fig. 6D). At longer time points significant increases in GlcCer labelling were detected probably due to the eventual storage of lysosomal GlcCer (Fig. 6D).

In order to understand the selectivity of cytosolic glycolipid transport we next studied traffic of galactosylceramide (GalCer) to the cell surface. The results were initially similar to those obtained with GlcCer: BFA inhibited transport of GalCer to the cell surface by 30-40% consistent with significant non-vesicular transport from the ER/Golgi to the cell surface; U18666A also inhibited GalCer transport by ~30% in the absence of BFA. However, in contrast to GlcCer, GalCer transport was not inhibited by U18666A in the presence of BFA (Fig. 6B) suggesting that U18666A inhibits vesicular but not non-vesicular GalCer transport. Control experiments showed that BFA was effective in inhibiting vesicular transport as it completely inhibited movement of GM3; U18666A also reduced surface GM3 consistent with inhibition of vesicular transport (Fig. S7).

## Discussion

We discovered defects in NPC cell culture models (increased endolysosomal pH and aberrant endocytic trafficking) consistent with a reduction in the cytosolic pool of GlcCer. Accordingly increasing cytosolic GlcCer by specifically inhibiting non-lysosomal glucocerebrosidase (GBA2) corrected both errors. This work consequently suggests GBA2 and vATPase as new therapeutic targets in NPCD. GlcCer has previously been suggested as a potential modulator of vATPase [7]. However previous studies have exclusively referred to melanocytes which are a specialised cell type with a particularly low Golgi and lysosomal pH needed for correct sorting to melanosomes. The generality of previous findings

or the application to human disease has not been previously addressed. The current study raises the question of how cytosolic GlcCer can be integrated with current understanding of NPC1 function. We wish to present two possible interpretations of these results.

The first interpretation relies on the classical role of NPC1 as a cholesterol export protein. Soluble partner protein NPC2 transfers the lipid to NPC1 from where it can transfer to the ER, via a partner protein. Since NPC2 can transfer cholesterol to membranes in the absence of NPC1 [59,60], and cholesterol is generally believed to flip between membrane leaflets with ease [61] dysfunctional NPC1 may reduce lysosome-ER trafficking and enrich the cytosolic leaflet of the endolysosome membrane in cholesterol. Within that leaflet cholesterol can be glycosylated by GBA2 using GlcCer, likely the major sphingolipid on the lysosomal surface, as a glucose donor. Thus NPC1 dysfunction will decrease GlcCer on the lysosomal surface in order to increase GlcChol [45]. Constant GlcCer levels during our experiments with U18666A (Fig. 6D) and modest elevations of GBA2 in NPCD mice [41] perhaps make this explanation less likely. However we cannot rule out increased degradation of a minor cytosolic GlcCer pool due to an increase in cholesterol levels.

Secondly, since inhibiting NPC1 function reduces cell surface transport (Fig. 6A,C) NPC1 may act as a GlcCer flippase [56] alone or in concert with another protein eg TMEM97 [62] or LAMP2 [63]. The region of NPC1 traditionally known as the sterol sensing domain (SSD) has significant sequence and structural similarity with transporters from the Resistance-Nodulation-Cell Division family [64,65] and can potentially bind mycolic acids [66]. It may therefore be large enough to accommodate other lipids, including GlcCer. The question remains of the precise role of U18666A in reducing transport of GlcCer, though not GalCer. Whilst this study did not address this, it could inhibit either non-vesicular transport or flipping. It has been reported on spectroscopic and crystallographic grounds that GalCer and GlcCer may share the same transfer proteins GLTP and FAPP2 [67,68], in which case U18666A specifically inhibits GlcCer flipping.

By whatever mechanism cytosolic GlcCer levels are controlled, this lipid may bind to and activate the vATPase [7,10,21] ensuring correct acidification, leading in turn to a functional endocytic pathway [35–38]. Whilst our findings point to this hypothesis further experiments will be necessary to confirm it, including investigations of whether other GlcCer binding proteins are involved, eg Galectin-3 which forms endocytic carrier structures in a GSL-dependent manner [69]. In NPC disease, levels of cytosolic GlcCer are reduced leading to impaired acidification and disrupted BODIPY-LacCer transport to a near-neutral compartment. The deficit of GlcCer at the cytosolic face of endolysosomes can be repaired by the addition of a GBA2 inhibitor. Reduced GlcCer levels have previously been associated with disrupted endocytic trafficking [10,15]. Our putative understanding is summarised in Fig. S8.

Other interpretations are less likely. The selectivity of U18666A inhibition of GlcCer transport could be explained by inducing GlcCer storage. However: 1) the presence of Brefeldin A in these experiments blocks vesicular transport and so newly synthesised cytoplasmic GlcCer wouldn't be expected to be stored; 2) U18666A-does not induce changes in GlcCer in the timeframe of the experiment (Fig. 6D). Decreased cell surface GlcCer could also be explained by lower endosomal recycling. However this explanation cannot adequately account for the selectivity we observe for GlcCer over GalCer (Fig. 6A, B).

Strong support for our interpretation would be derived from directly measured changes in levels of cytosolic GlcCer and these changes correlating with lysosomal function. Unfortunately such a direct measurement is not currently possible. The best available surrogate is to measure GlcCer at the cellular level. In healthy cells treatment with AMP-DNJ does not result in changes to whole cell GlcCer (Fig. S4) despite this compound being a potent GBA2 inhibitor ($IC_{50}$ ~ 1nM [42]). We suggest that this is because AMP-DNJ acts only on a minor pool of GlcCer and so gives changes which are undetectable at the cellular level. In contrast, in NPCD cells GlcCer levels are elevated (Fig. S4) and doses of 1-20nM AMP-DNJ lead to further increased GlcCer. We believe that when our data is taken together, especially that concerning the use of 1μM NB-DNJ, 6 μM NB-DGJ and brefeldin A (cytoplasmic GlcCer increases in ER/Golgi),

increased GlcCer is the best explanation. Overall 5-10nM AMP-DNJ would be recommended based on experiments in a variety of cell types (data not shown).

Other pathways involving lipids and regulating endolysosomal pH also operate. 1) sorting of vATPase via FAPP2-mediated recycling of non-vATPase containing tubules [70] and endocytic maturation involves the sorting and activation of the vATPase [21,71,72]. 2) GlcCer binding to the mTORC1/ragulator complex which is a key regulator of vATPase [9]. Evidence for this possibility also includes the observation the GlcCer precursors palmitate, serine and glucose, as well as GlcCer itself, are all implicated in the regulation of mTORC1 [73,74]. The relationship between NPC1 and mTOR requires further elucidation as cholesterol accumulation has variously been reported to result in mTORC1 inhibition [75], mTORC1 activation [76] and no difference in mTORC1 status [77]. 3) association between NPC1 and components of the vATPase [76,78]. 4) the potential involvement of GlcSph, although this is less likely here as GBA2 inhibition does not correct GlcSph elevation [41,79,80]. 5) the possibility that NPC1 exports sphingosine [5,81,82], reported as an endogenous inhibitor of GBA2 [83]; recent molecular modelling work from our laboratory supports this [84]. 6) accumulating lipids permeabilise the lysosome [85–88] which would be expected to lead to proton leak.

It is commonly thought that increasing pH will inevitably result in dysfunction of lysosomal hydrolases. In fact approximately half of such enzymes, not least most of the cathepsin family, have pH optima of 5 or above [89]. Thus the pH increase reported here will not in itself lead to widespread failure of lysosomal catabolism. Consistently, vATPase inhibition does not increase lysosomal amino acids [90]. Instead lysosomal hydrolases with low pH optima and high substrate flux, such as lysosomal acid lipase, will be affected as previously reported [7,10,12,91].

It is important to consider the details of the measurement of endolysosomal pH. As noted, various results have been reported and it's possible that some of the confusion regarding pH in NPCD cells is due to different techniques measuring different compartments. We do not consider our data to be in direct conflict with some previous reports of no increase in *lysosomal* pH in NPCD cells as measured by other probes. We subscribe to the popular view that lysosomal storage diseases are a 'traffic jam' [92,93]. Thus results with our probe, which reports a single value for the combination of endosomal and lysosomal pH, represent delayed endolysosomal acidification, and do not preclude mature lysosomes fully acidifying. This explains why our results are different to those using other probes, and also to those gained using LysoTracker red [23] as fluorescence from this probe (pKa 7.5) is not sensitive to pH changes below about 6.5 [94]. Differing reported pH values are thus a reflection of differing experimental techniques measuring different compartments.

It is not known why different pools of GlcCer have opposite effects on endolysosomal pH. GlcCer storage within the lysosome increases endolysosomal pH [10–13,20] whereas increasing *cytosolic* GlcCer decreases pH (current study). Possibly different pools of GlcCer bind different vATPase domains with opposite effects. It is also possible that overexpression of GBA2, which occurs both in Gaucher and NPC disease, increases the degradation of cytosolic GlcCer. New techniques that are able to measure different pools of GlcCer will be needed to address this issue.

In summary we have found defects in NPCD cells consistent with a reduced cytosolic pool of GlcCer and demonstrated the repair of these defects by inhibiting cytosolic GlcCer breakdown. This led in turn to further evidence that GlcCer may bind vATPase a subunit which may show decreased expression and could explain increased endolysosomal pH in GlcCer synthase knockout cells. Our findings are consistent with studies in mouse models of NPCD [95] as well as other LSDs [96,97] where miglustat was found to be disease-modifying despite increased levels of brain GlcCer, which is inconsistent with synthase inhibition. We think it is significant that recent reports point to a key role for lysosomal acidification in LSDs and neurodegenerative diseases more generally [13,98,99]. GBA2 and vATPase are therefore potential drug targets for NPCD and other diseases of lysosomal dysfunction.

**Experimental Procedures**

**Materials** were obtained from Sigma unless otherwise indicated. Tissue culture media and supplements were from Gibco. Foetal Calf Serum (FCS) was from PAA laboratories. LysoSensor yellow/blue, BODIPY-LacCer and LysoTracker red were from Invitrogen. U18666A was from Affinity Research Chemicals (Exeter, UK). Brefeldin A was from Cayman Chemical. AMP-DNJ was prepared as previously described [43].

**Cell culture** Normal and storing patient lymphoblasts and fibroblasts (GM03124 (mutation P237S), GM03299, GM03123 (mutation P237S), GM05399 and GM00380) were obtained from the Coriell Institute, Human Genetic Mutant Cell Repository (New Jersey, USA). RAW 264.1 mouse macrophages were obtained from the ECACC (Porton Down, UK). HAP1 cells (wt and GBA2 KO) were obtained from Horizon (Cambridge, UK). Cells were maintained in RPMI (lymphoblasts and RAWs), DMEM (fibroblasts, CHOs) or IMDM (HAP1s) supplemented with 10 mM glutamine, 50 U/ml penicillin / streptomycin and 10% FCS. U18666A was at a final concentration of 5 µM, dissolved in ethanol at 1000x concentration and stored at –20˚C. AMP-DNJ (AMP-DNJ) was added at 1-20nM and was dissolved in DMSO at 500x concentration and stored at –20˚C.

**Fluorescence microscopy** Cells were placed on glass coverslips and left to adhere overnight. Cells were labelled by pulsing with BODIPY-$C_5$-LacCer in medium containing 1% serum for 30-60 minutes, removing cell surface fluorescence by washing 3 times for 1-5 minutes and chasing for 60-90 minutes (15). Fluorescent cells were observed using Leica or EVOS fluorescence microscopes. BODIPY was excited at 450-490 nm and viewed at >520 nm. BODIPY-TR and LysoTracker were excited at 530-540nm and viewed at >560nm. Pearson's coefficients were calculated using the Image J JACoP plugin.

Golgi targeting can be assessed by co-localisation with a Golgi marker, eg BODIPY-TR ceramide (see Fig 4).

**Endolysosomal pH measurement** Experiments with acridine orange were performed as previously described [18]. Typically 10-15 Images were collected from 3 separate experiments and the red green ratio of the (200-500) punctates were calculated using Image J.

Endolysosomal pH was also determined using LysoSensor yellow/blue [30,100] using a previously published method [101].

**GLTP surface assay** was as described by [56].

**Lipid analysis:** Lipids were extracted and applied to TLC plates, which, when used to separate GalCer from GlcCer, had been dipped in 2.5% wt/vol boric acid in MeOH and dried. Lipids were generally separated by 2D TLC using either $CHCl_3$/MeOH/25% vol/vol $NH_4OH$/water (65:35:4:4 vol/vol) or $CHCl_3$/MeOH/0.2% aqueous $CaCl_2$ (55:45:10 vol/vol) for the first dimension $CHCl_3$/MeOH/acetone/HOAc/water (50:20:10:10:5 vol/vol) for the second dimension. Radiolabelled spots were detected by exposure of phosphorimaging screens and read-out on a Personal FX phosphorimager. TLC plates with fluorescent lipids were directly developed using a phosphorimager (STORM 860; Molecular Dynamics). Spots were identified by comparison with standards and quantified using Quantity One software (Bio-Rad Laboratories).

GlcCer quantitation was performed as previously described [102].

**Molecular modelling**: A model for the a and c subunit of vATPase where no experimental structure is available was constructed using SwissModel using 5TJ5 [47] (67% identical, downloaded from the PDB) as a template [48,49]. Docking of GlcCer headgroup was conducted using ROSIE (rosie.rosettacommons.org) [51–53]. All settings were defaults; NZ of Lys54 (subunit c) was used as the starting position. ROSIE output was visualised using UCSF Chimera [103].

**PCR**: All cultured cells were prepared immediately before RNA extraction. Total RNA was extracted using RNeasy mini kit (Qiagen) and final RNA pellets were re-suspended in PCR grade water. The RNA purity was crudely assessed using a Nanodrop (ThermoFisher) which gave a 260/280nm ratio of 1.9-2.1 for all samples. cDNA was synthesized from 1µg of RNA using SensiFast cDNA Synthesis Kit (BioLine, London, UK). Quantitative RT-PCR was performed using SensiFast SYBR® Hi-Rox kit assays in a StepOne instrument. The thermal profile was 2 min at 95°C, 40 cycles of 5 s at 95°C, and 30 sec at 58°C. Non-template controls were included for all samples. Results were expressed as expression relative to TATA box binding protein (TBP) $2^{-\Delta ct}$ (mean±SD)

Primers: human ATP6V0A1 (NM_001130020.1),. TBP was used as a housekeeping gene.

**Sequence alignment:** this was performed in Clustal Omega [104] and results visualised in Jalview [105].

**Statistical analysis**: results are presented as mean±SEM in the text and mean ±SD in the figures unless otherwise stated. Statistical significance was assessed using Student's one- or two-tailed t-tests and two-way ANOVA calculated using Microsoft Excel.

**Acknowledgements:** We thank De Montfort University (to SW/DJS), Beyond Batten Disease Foundation (NS/DJS) the European Council (grant MRTN-CT-2004-5330, to DH/HS) and VKS-GVN (to MF/JA) for financial support. We are grateful to Profs Frances Platt (Oxford University) and Dagmar Wachten (CAESAR, Bonn) for gifts of cells and to Dr Stephen Muench (Leeds University) for helpful discussions.

**Conflict of interest:** The authors declare they have no conflicts of interest with the contents of this article.

(1) Puri, V.; Watanabe, R.; Dominguez, M.; Sun, X.; Wheatley, C. L.; Marks, D. L.; Pagano, R. E. Cholesterol Modulates Membrane Traffic along the Endocytic Pathway in Sphingolipid-Storage Diseases. *Nat. Cell Biol.* **1999**, *1* (6), 386–388.

(2) Sugimoto, Y.; Ninomiya, H.; Ohsaki, Y.; Higaki, K.; Davies, J. P.; Ioannou, Y. A.; Ohno, K. Accumulation of Cholera Toxin and GM1 Ganglioside in the Early Endosome of Niemann-Pick C1-Deficient Cells. *Proc. Natl. Acad. Sci.* **2001**, *98* (22), 12391–12396.

(3) Higgins, M. E.; Davies, J. P.; Chen, F. W.; Ioannou, Y. A. Niemann–Pick C1 Is a Late Endosome-Resident Protein That Transiently Associates with Lysosomes and the Trans-Golgi Network. *Mol. Genet. Metab.* **1999**, *68* (1), 1–13.

(4) Shen, D.; Wang, X.; Li, X.; Zhang, X.; Yao, Z.; Dibble, S.; Dong, X.; Yu, T.; Lieberman, A. P.; Showalter, H. D.; et al. Lipid Storage Disorders Block Lysosomal Trafficking by Inhibiting a TRP Channel and Lysosomal Calcium Release. *Nat. Commun.* **2012**, *3*, 731.

(5) Lloyd-Evans, E.; Morgan, A. J.; He, X.; Smith, D. A.; Elliot-Smith, E.; Sillence, D. J.; Churchill, G. C.; Schuchman, E. H.; Galione, A.; Platt, F. M. Niemann-Pick Disease Type C1 Is a Sphingosine Storage Disease That Causes Deregulation of Lysosomal Calcium. *Nat. Med.* **2008**, *14*, 1247–1255.

(6) Shen, W.; Henry, A. G.; Paumier, K. L.; Li, L.; Mou, K.; Dunlop, J.; Berger, Z.; Hirst, W. D. Inhibition of Glucosylceramide Synthase Stimulates Autophagy Flux in Neurons. *J. Neurochem.* **2014**, *129* (5), 884–894.

(7) van der Poel, S.; Wolthoorn, J.; van den Heuvel, D.; Egmond, M.; Groux-Degroote, S.; Neumann, S.; Gerritsen, H.; van Meer, G.; Sprong, H. Hyperacidification of Trans-Golgi Network and Endo/Lysosomes in Melanocytes by Glucosylceramide-Dependent V-ATPase Activity. *Traffic* **2011**, *12* (11), 1634–1647.

(8) Yamaguchi, M.; Kasamo, K. Modulation in the Activity of Purified Tonoplast H+-ATPase by Tonoplast Glycolipids Prepared from Cultured Rice (Oryza Sativa L. Var. Boro) Cells. *Plant Cell Physiol.* **2001**, *42* (5), 516–523.

(9) Zhu, H.; Shen, H.; Sewell, A. K.; Kniazeva, M.; Han, M. A Novel Sphingolipid-TORC1 Pathway Critically Promotes Postembryonic Development in Caenorhabditis Elegans. *Elife* **2013**, *2:e00429.*, e00429.

(10) Sillence, D. J. Glucosylceramide Modulates Endolysosomal PH in Gaucher Disease. *Mol. Genet. Metab.* **2013**, *109* (2), 194–200.

(11) De La Mata, M.; Cotán, D.; Oropesa-Ávila, M.; Villanueva-Paz, M.; De Lavera, I.; Álvarez-Córdoba, M.; Luzón-Hidalgo, R.; Suárez-Rivero, J. M.; Tiscornia, G.; Sánchez-Alcázar, J. A. Coenzyme Q10 Partially Restores Pathological Alterations in a Macrophage Model of Gaucher Disease. *Orphanet J. Rare Dis.* **2017**, *12* (1), 1–15.

(12) Magalhaes, J.; Gegg, M. E.; Migdalska-Richards, A.; Doherty, M. K.; Whitfield, P. D.; Schapira, A. H. V. Autophagic Lysosome Reformation Dysfunction in Glucocerebrosidase Deficient Cells: Relevance to Parkinson Disease. *Hum. Mol. Genet.* **2015**, *25* (16), 3432–3445.

(13) Bourdenx, M.; Daniel, J.; Genin, E.; Soria, F. N.; Blanchard-Desce, M.; Bezard, E.; Dehay, B. Nanoparticles Restore Lysosomal Acidification Defects: Implications for Parkinson and Other Lysosomal-Related Diseases. *Autophagy* **2016**, *12* (3), 472–483.

(14) Yamashita, T.; Wada, R.; Sasaki, T.; Deng, C.; Bierfreund, U.; Sandhoff, K.; Proia, R. L. A Vital Role for Glycosphingolipid Synthesis during Development and Differentiation. *Proc. Natl. Acad. Sci.* **1999**, *96* (16), 9142–9147.

(15) Sillence, D. J.; Puri, V.; Marks, D. L.; Butters, T. D.; Dwek, R. A.; Pagano, R. E.; Platt, F. M. Glucosylceramide Modulates Membrane Traffic along the Endocytic Pathway. *J. Lipid Res.* **2002**, *43* (11), 1837–1845.

(16) Brett, C. L.; Kallay, L.; Hua, Z.; Green, R.; Chyou, A.; Zhang, Y.; Graham, T. R.; Donowitz, M.; Rao, R. Genome-Wide Analysis Reveals the Vacuolar pH-Stat of Saccharomyces Cerevisiae. *PLoS One* **2011**, *6* (3), e17619.

(17) Malathi, K.; Higaki, K.; Tinkelenberg, A. H.; Balderes, D. A.; Almanzar-Paramio, D.; Wilcox, L. J.; Erdeniz, N.; Redican, F.; Padamsee, M.; Liu, Y.; et al. Mutagenesis of the Putative Sterol-Sensing Domain of Yeast Niemann Pick C–related Protein Reveals a Primordial Role in Subcellular Sphingolipid Distribution. *J. Cell Biol.* **2004**, *164* (4), 547–556.

(18) Bach, G.; Chen, C.-S.; Pagano, R. E. Elevated Lysosomal pH in Mucolipidosis Type IV Cells. *Clin. Chim. Acta* **1999**, *280* (1–2), 173–179.

(19) Tharkeshwar, A. K.; Trekker, J.; Vermeire, W.; Pauwels, J.; Sannerud, R.; Priestman, D. A.; Te Vruchte, D.; Vints, K.; Baatsen, P.; Decuypere, J.-P.; et al. A Novel Approach to Analyze Lysosomal Dysfunctions through Subcellular Proteomics and Lipidomics: The Case of NPC1 Deficiency. *Sci. Rep.* **2017**, *7*, 41408.

(20) Chakraborty, K.; Leung, K.; Krishnan, Y. High Lumenal Chloride in the Lysosome Is Critical for Lysosome Function. *Elife* **2017**, *6*, e28862.

(21) Lafourcade, C. C.; Sobo, K.; Kieffer-Jaquinod, S.; Garin, J. J.; van, der G.; van der Goot, F. G. Regulation of the V-ATPase along the Endocytic Pathway Occurs through Reversible Subunit Association and Membrane Localization. *PLoS One* **2008**, *3* (7), e2758.

(22) Lu, F.; Liang, Q.; Abi-Mosleh, L.; Das, A.; De Brabander K., J.; Goldstein, J. L.; Brown, M. S. Identification of NPC1 as the Target of U18666A, an Inhibitor of Lysosomal Cholesterol Export and Ebola Infection. *Elife* **2015**, *4*, e12177.

(23) Shoemaker, C. J.; Schornberg, K. L.; Delos, S. E.; Scully, C.; Pajouhesh, H.; Olinger, G. G.; Johansen, L. M.; White, J. M. Multiple Cationic Amphiphiles Induce a Niemann-Pick C Phenotype and Inhibit Ebola Virus Entry and Infection. *PLoS One* **2013**, *8*, e56265.

(24) Ng, M.; Ndungo, E.; Jangra, R. K.; Cai, Y.; Postnikova, E.; Radoshitzky, S. R.; Dye, J. M.; Ramírez de Arellano, E.; Negredo, A.; Palacios, G.; et al. Cell Entry by a Novel European Filovirus Requires Host Endosomal Cysteine Proteases and Niemann-Pick C1. *Virology* **2014**, *468*, 637–646.

(25) Johansen, L. M.; Brannan, J. M.; Delos, S. E.; Shoemaker, C. J.; Stossel, A.; Lear, C.; Hoffstrom, B. G.; DeWald, L. E.; Schornberg, K. L.; Scully, C.; et al. FDA-Approved Selective Estrogen Receptor Modulators Inhibit Ebola Virus Infection. *Sci. Transl. Med.* **2013**, *5* (190), 190ra79.

(26) Funk, R. S.; Krise, J. P. Cationic Amphiphilic Drugs Cause a Marked Expansion of Apparent

Lysosomal Volume: Implications for an Intracellular Distribution-Based Drug Interaction. *Mol. Pharm.* **2012**, *9* (5), 1384–1395.

(27) te Vruchte, D.; Speak, A. O.; Wallom, K. L.; Al Eisa, N.; Smith, D. A.; Hendriksz, C. J.; Simmons, L.; Lachmann, R. H.; Cousins, A.; Hartung, R.; et al. Relative Acidic Compartment Volume as a Lysosomal Storage Disorderâ€“associated Biomarker. *J. Clin. Invest.* **2014**, *124* (3), 1320–1328.

(28) Xu, M.; Liu, K.; Swaroop, M.; Porter, F. D.; Sidhu, R.; Finkes, S.; Ory, D. S.; Marugan, J. J.; Xiao, J.; Southall, N.; et al. D-Tocopherol Reduces Lipid Accumulation in Niemann-Pick Type C1 and Wolman Cholesterol Storage Disorders. *J. Biol. Chem.* **2012**, *287* (47), 39349–39360.

(29) Wang, R.; Hosaka, M.; Han, L.; Yokota-Hashimoto, H.; Suda, M.; Mitsushima, D.; Torii, S.; Takeuchi, T. Molecular Probes for Sensing the Cholesterol Composition of Subcellular Organelle Membranes. *Biochim. Biophys. Acta* **2006**, *1761* (10), 1169–1181.

(30) Diwu, Z.; Chen, C.-S.; Zhang, C.; Klaubert, D. H.; Haugland, R. P. A Novel Acidotropic pH Indicator and Its Potential Application in Labeling Acidic Organelles of Live Cells. *Chem. Biol.* **1999**, *6* (7), 411–418.

(31) Otomo, T.; Higaki, K.; Nanba, E.; Ozono, K.; Sakai, N. Lysosomal Storage Causes Cellular Dysfunction in Mucolipidosis II Skin Fibroblasts. *J. Biol. Chem.* **2011**, *286* (40), 35283–35290.

(32) Coffey, E. E.; Beckel, J. M.; Laties, A. M.; Mitchell, C. H. Lysosomal Alkalization and Dysfunction in Human Fibroblasts with the Alzheimer's Disease-Linked Presenilin 1 A246E Mutation Can Be Reversed with cAMP. *Neuroscience* **2014**, *263*, 111–124.

(33) Pryor, P. R.; Reimann, F.; Gribble, F. M.; Luzio, J. P. Mucolipin-1 Is a Lysosomal Membrane Protein Required for Intracellular Lactosylceramide Traffic. *Traffic* **2006**, *7* (10), 1388–1398.

(34) Choudhury, A.; Dominguez, M.; Puri, V.; Sharma, D. K.; Narita, K.; Wheatley, C. L.; Marks, D. L.; Pagano, R. E. Rab Proteins Mediate Golgi Transport of Caveola-Internalized Glycosphingolipids and Correct Lipid Trafficking in Niemann-Pick C Cells. *J. Clin. Invest.* **2002**, *109* (12), 1541–1550.

(35) Baravalle, G.; Schober, D.; Huber, M.; Bayer, N.; Murphy, R. F.; Fuchs, R. Transferrin Recycling and Dextran Transport to Lysosomes Is Differentially Affected by Bafilomycin, Nocodazole, and Low Temperature. *Cell Tissue Res.* **2005**, *320* (1), 99–113.

(36) Bayer, N.; Schober, D.; Prchla, E.; Murphy, R. F.; Blaas, D.; Fuchs, R. Effect of Bafilomycin A1 and Nocodazole on Endocytic Transport in HeLa Cells: Implications for Viral Uncoating and Infection. *J. Virol.* **1998**, *72* (12), 9645–9655.

(37) Clague, M. J.; Urbé, S.; Aniento, F.; Gruenberg, J. Vacuolar ATPase Activity Is Required for Endosomal Carrier Vesicle Formation. *J. Biol. Chem.* **1994**, *269* (1), 21–24.

(38) van Weert, A. W.; Dunn, K. W.; Gueze, H. J.; Maxfield, F. R.; Stoorvogel, W. Transport from Late Endosomes to Lysosomes, but Not Sorting of Integral Membrane Proteins in Endosomes, Depends on the Vacuolar Proton Pump. *J. Cell Biol.* **1995**, *130* (4), 821–834.

(39) Chen, C.-S.; Patterson, M. C.; O'Brien, J. F.; Pagano, R. E.; Wheatley, C. L. Broad Screening Test for Sphingolipid-Storage Diseases. *Lancet* **1999**, *354* (9182), 901–905.

(40) Warnock, D. E.; Lutz, M. S.; Blackburn, W. A.; Young, W. W.; Baenziger, J. U. Transport of Newly Synthesized Glucosylceramide to the Plasma-Membrane by a Non-Golgi Pathway. *Proc. Natl. Acad. Sci. U. S. A.* **1994**, *91* (7), 2708–2712.

(41) Marques, A. R. A.; Aten, J.; Ottenhoff, R.; van Roomen, C. P. A. A.; Herrera Moro, D.; Claessen, N.; Vinueza Veloz, M. F.; Zhou, K.; Lin, Z.; Mirzaian, M.; et al. Reducing GBA2 Activity Ameliorates

Neuropathology in Niemann-Pick Type C Mice. *PLoS One* **2015**, *10* (8), e0135889.

(42) Ridley, C. M.; Thur, K. E.; Shanahan, J.; Thillaiappan, N. B.; Shen, A.; Uhl, K.; Walden, C. M.; Rahim, A. A.; Waddington, S. N.; Platt, F. M.; et al. Beta-Glucosidase 2 (GBA2) Activity and Imino Sugar Pharmacology. *J. Biol. Chem.* **2013**.

(43) Overkleeft, H. S.; Renkema, G. H.; Neele, J.; Vianello, P.; Hung, I. O.; Strijland, A.; van der Burg, A. M.; Koomen, G.-J.; Pandit, U. K.; Aerts, J. M. F. G. Generation of Specific Deoxynojirimycin-Type Inhibitors of the Non-Lysosomal Glucosylceramidase. *J. Biol. Chem.* **1998**, *273* (41), 26522–26527.

(44) Dekker, N.; Voorn-Brouwer, T.; Verhoek, M.; Wennekes, T.; Narayan, R. S.; Speijer, D.; Hollak, C. E. M.; Overkleeft, H. S.; Boot, R. G.; Aerts, J. M. F. G. The Cytosolic β-Glucosidase GBA3 Does Not Influence Type 1 Gaucher Disease Manifestation. *Blood Cells, Mol. Dis.* **2011**, *46* (1), 19–26.

(45) Marques, A. R. A.; Mirzaian, M.; Akiyama, H.; Wisse, P.; Ferraz, M. J.; Gaspar, P.; Ghauharali-van der Vlugt, K.; Meijer, R.; Giraldo, P.; Alfonso, P.; et al. Glucosylated Cholesterol in Mammalian Cells and Tissues: Formation and Degradation by Multiple Cellular ß-Glucosidases. *J. Lipid Res.* **2016**, *57* (3), 451–463.

(46) Zhu, H.; Sewell, A. K.; Han, M. Intestinal Apical Polarity Mediates Regulation of TORC1 by Glucosylceramide in C. Elegans. *Genes Dev.* **2015**, *29* (12), 1218–1223.

(47) Mazhab-Jafari, M.; Rohou, A.; Schmidt, C.; Bueler, S. A.; Benlekbir, S.; Robinson, C. V; Rubinstein, J. L. Atomic Model for the Membrane-Embedded VO Motor of a Eukaryotic V-ATPase. *Nature* **2016**, *539* (7627), 118–122.

(48) Arnold, K.; Bordoli, L.; Kopp, J.; Schwede, T. The SWISS-MODEL Workspace: A Web-Based Environment for Protein Structure Homology Modelling. *Bioinformatics* **2006**, *22* (2), 195–201.

(49) Biasini, M.; Bienert, S.; Waterhouse, A.; Arnold, K.; Studer, G.; Schmidt, T.; Kiefer, F.; Cassarino, T. G.; Bertoni, M.; Bordoli, L.; et al. SWISS-MODEL: Modelling Protein Tertiary and Quaternary Structure Using Evolutionary Information. *Nucleic Acids Res.* **2014**, *42* (W1), W252–W258.

(50) Studer, G.; Biasini, M.; Schwede, T. Assessing the Local Structural Quality of Transmembrane Protein Models Using Statistical Potentials (QMEANBrane). *Bioinformatics* **2014**, *30* (17), i505–i511.

(51) Lyskov, S.; Chou, F.-C.; Conchúr, S. Ó.; Der, B. S.; Drew, K.; Kuroda, D.; Xu, J.; Weitzner, B. D.; Renfrew, P. D.; Sripakdeevong, P.; et al. Serverification of Molecular Modeling Applications: The Rosetta Online Server That Includes Everyone (ROSIE). *PLoS One* **2013**, *8* (5), e63906.

(52) Lyskov, S.; Gray, J. J. The RosettaDock Server for Local Protein-Protein Docking. *Nucleic Acids Res.* **2008**, *36* (Web Server issue), W233–W238.

(53) Combs, S. A.; DeLuca, S. L. S. H. S. L.; DeLuca, S. L. S. H. S. L.; Lemmon, G. H.; Nannemann, D. P.; Nguyen, E. D.; Willis, J. R.; Sheehan, J. H.; Meiler, J. Small-Molecule Ligand Docking into Comparative Models with Rosetta. *Nat.Protocols* **2013**, *8* (7), 1277–1298.

(54) van der Poel, S. Regulation of Organelle pH by Glycoshingolipids, University of Utrecht: Utrecht, 2010.

(55) Gorbitz, C. H.; Etter, M. C. Hydrogen Bonds to Carboxylate Groups. Syn/Anti Distributions and Steric Effects. *J. Am. Chem. Soc.* **1992**, *114* (2), 627–631.

(56) Halter, D.; Neumann, S.; van Dijk, S. M.; Wolthoorn, J.; de Mazière, A. M.; Vieira, O. V; Mattjus, P.; Klumperman, J.; van Meer, G.; Sprong, H. Pre- and Post-Golgi Translocation of Glucosylceramide in Glycosphingolipid Synthesis. *J. Cell Biol.* **2007**, *179* (1), 101–115.

(57) D'Angelo, G.; Uemura, T.; Chuang, C. C.; Polishchuk, E.; Santoro, M.; Ohvo-Rekilä, H.; Sato, T.; Di Tullio, G.; Varriale, A.; D'Auria, S.; et al. Vesicular and Non-Vesicular Transport Feed Distinct Glycosylation Pathways in the Golgi. *Nature* **2013**, *501* (7465), 116–120.

(58) D'Angelo, G.; Polishchuk, E.; Tullio, G. Di; Santoro, M.; Campli, A. Di; Godi, A.; West, G.; Bielawski, J.; Chuang, C. C.; Van Der Spoel, A. C.; et al. Glycosphingolipid Synthesis Requires FAPP2 Transfer of Glucosylceramide. *Nature* **2007**, *449* (7158), 62–67.

(59) Cheruku, S. R.; Xu, Z.; Dutia, R.; Lobel, P.; Storch, J. Mechanism of Cholesterol Transfer from the Niemann-Pick Type C2 Protein to Model Membranes Supports a Role in Lysosomal Cholesterol Transport. *J. Biol. Chem.* **2006**, *281* (42), 31594–31604.

(60) Infante, R. E.; Wang, M. L.; Radhakrishnan, A.; Kwon, H. J.; Brown, M. S.; Goldstein, J. L. NPC2 Facilitates Bidirectional Transfer of Cholesterol between NPC1 and Lipid Bilayers, a Step in Cholesterol Egress from Lysosomes. *Proc. Natl. Acad. Sci.* **2008**, *105* (40), 15287–15292.

(61) Steck, T. L.; Ye, J.; Lange, Y. Probing Red Cell Membrane Cholesterol Movement with Cyclodextrin. *Biophys. J.* **2002**, *83* (4), 2118–2125.

(62) Bartz, F.; Kern, L.; Erz, D.; Zhu, M.; Gilbert, D.; Meinhof, T.; Wirkner, U.; Erfle, H.; Muckenthaler, M.; Pepperkok, R.; et al. Identification of Cholesterol-Regulating Genes by Targeted RNAi Screening. *Cell Metab.* **2009**, *10* (1), 63–75.

(63) Li, J.; Pfeffer, S. R. Lysosomal Membrane Glycoproteins Bind Cholesterol and Contribute to Lysosomal Cholesterol Export. *Elife* **2016**, *5*, e21635.

(64) Li, X.; Wang, J.; Coutavas, E.; Shi, H.; Hao, Q.; Blobel, G. Structure of Human Niemann–Pick C1 Protein. *Proc. Natl. Acad. Sci.* **2016**, *113* (29), 8212–8217.

(65) Davies, J. P.; Chen, F. W.; Ioannou, Y. A. Transmembrane Molecular Pump Activity of Niemann-Pick C1 Protein. *Science (80).* **2000**, *290*, 2295.

(66) Fineran, P.; Lloyd-Evans, E.; Lack, N. A.; Platt, N.; Davis, L. C.; Morgan, A. J.; Höglinger, D.; Tatituri, R. V. V; Clark, S.; Williams, I. M.; et al. Pathogenic Mycobacteria Achieve Cellular Persistence by Inhibiting the Niemann-Pick Type C Disease Cellular Pathway. *Wellcome Open Res.* **2016**, *1* (18).

(67) Malinina, L.; Malakhova, M. L.; Kanack, A. T.; Lu, M.; Abagyan, R.; Brown, R. E.; Patel, D. J. The Liganding of Glycolipid Transfer Protein Is Controlled by Glycolipid Acyl Structure. *PLoS Biol.* **2006**, *4* (11), 1996–2011.

(68) Samygina, V. R.; Ochoa-Lizarralde, B.; Popov, A. N.; Cabo-Bilbao, A.; Goni-de-Cerio, F.; Molotkovsky, J. G.; Patel, D. J.; Brown, R. E.; Malinina, L. Structural Insights into Lipid-Dependent Reversible Dimerization of Human GLTP. *Acta Crystallogr. Sect. D* **2013**, *69* (4), 603–616.

(69) Lakshminarayan, R.; Wunder, C.; Becken, U.; Howes, M. T.; Benzing, C.; Arumugam, S.; Sales, S.; Ariotti, N.; Chambon, V.; Lamaze, C.; et al. Galectin-3 Drives Glycosphingolipid-Dependent Biogenesis of Clathrin-Independent Carriers. *Nat. Cell Biol.* **2014**, *16* (6), 592–603.

(70) Cao, X.; Coskun, Ü.; Rössle, M.; Buschhorn, S. B.; Grzybek, M.; Dafforn, T. R.; Lenoir, M.; Overduin, M.; Simons, K. Golgi Protein FAPP2 Tubulates Membranes. *Proc. Natl. Acad. Sci.* **2009**, *106* (50), 21121–21125.

(71) Kane, P. M. The Where, When, and How of Organelle Acidification by the Yeast Vacuolar H+-ATPase. *Microbiol. Mol. Rev.* **2006**, *70* (1), 177–191.

(72) Trombetta, E. S.; Ebersold, M.; Garrett, W.; Pypaert, M.; Mellman, I. Activation of Lysosomal Function during Dendritic Cell Maturation. *Science (80).* **2003**, *299* (5611), 1400–1403.

(73) Bar-Peled, L.; Schweitzer, L. D.; Zoncu, R.; Sabatini, D. M. Ragulator Is a GEF for the Rag GTPases That Signal Amino Acid Levels to MTORC1. *Cell* **2012**, *150* (6), 1196–1208.

(74) Zoncu, R.; Bar-Peled, L.; Efeyan, A.; Wang, S.; Sancak, Y.; Sabatini, D. M. MTORC1 Senses Lysosomal Amino Acids through an Inside-out Mechanism That Requires the Vacuolar H(+)-ATPase. *Science (80-. ).* **2011**, *334* (6056), 678–683.

(75) Xu, J.; Dang, Y.; Ren, Y. R.; Liu, J. O. Cholesterol Trafficking Is Required for MTOR Activation in Endothelial Cells. *Proc. Natl. Acad. Sci.* **2010**, *107* (10), 4764–4769.

(76) Castellano, B. M.; Thelen, A. M.; Moldavski, O.; Feltes, M.; van der Welle, R. E. N.; Mydock-McGrane, L.; Jiang, X.; van Eijkeren, R. J.; Davis, O. B.; Louie, S. M.; et al. Lysosomal Cholesterol Activates MTORC1 via an SLC38A9-Niemann-Pick C1 Signaling Complex. *Science* **2017**, *355* (6331), 1306–1311.

(77) Pacheco, C. D.; Kunkel, R.; Lieberman, A. P. Autophagy in Niemann–Pick C Disease Is Dependent upon Beclin-1 and Responsive to Lipid Trafficking Defects. *Hum. Mol. Genet.* **2007**, *16* (12), 1495–1503.

(78) Macías-Vidal, J.; Guerrero-Hernández, M.; Estanyol, J. M.; Aguado, C.; Knecht, E.; Coll, M. J.; Bachs, O. Identification of Lysosomal Npc1-Binding Proteins: Cathepsin D Activity Is Regulated by NPC1. *Proteomics* **2016**, *16* (1), 150–158.

(79) Mistry, P. K.; Liu, J.; Sun, L.; Chuang, W.-L.; Yuen, T.; Yang, R.; Lu, P.; Zhang, K.; Li, J.; Keutzer, J.; et al. Glucocerebrosidase 2 Gene Deletion Rescues Type 1 Gaucher Disease. *Proc. Natl. Acad. Sci.* **2014**, *111* (13), 4934–4939.

(80) Hamler, R.; Brignol, N.; Clark, S. W.; Morrison, S.; Dungan, L. B.; Chang, H. H.; Khanna, R.; Frascella, M.; Valenzano, K. J.; Benjamin, E. R.; et al. Glucosylceramide and Glucosylsphingosine Quantitation by Liquid Chromatography-Tandem Mass Spectrometry to Enable in Vivo Preclinical Studies of Neuronopathic Gaucher Disease. *Anal. Chem.* **2017**, *89* (16), 8288–8295.

(81) Höglinger, D.; Haberkant, P.; Aguilera-Romero, A.; Riezman, H.; Porter, F. D.; Platt, F. M.; Galione, A.; Schultz, C. Intracellular Sphingosine Releases Calcium from Lysosomes. *Elife* **2015**, *4*, 4:e10616.

(82) Höglinger, D.; Nadler, A.; Haberkant, P.; Kirkpatrick, J.; Schifferer, M.; Stein, F.; Hauke, S.; Porter, F. D.; Schultz, C. Trifunctional Lipid Probes for Comprehensive Studies of Single Lipid Species in Living Cells. *Proc. Natl. Acad. Sci.* **2017**, *114* (7), 1566–1571.

(83) Schonauer, S.; Körschen, H. G.; Penno, A.; Rennhack, A.; Breiden, B.; Sandhoff, K.; Gutbrod, K.; Dörmann, P.; Raju, D. N.; Haberkant, P.; et al. Identification of a Feedback Loop Involving Beta-Glucosidase 2 and Its Product Sphingosine Sheds Light on the Molecular Mechanisms in Gaucher Disease. *J. Biol. Chem.* **2017**.

(84) Wheeler, S.; Schmid, R.; Sillence, D. J. Lipid–Protein Interactions in Niemann–Pick Type C Disease: Insights from Molecular Modeling. *Int. J. Mol. Sci. 2019, Vol. 20, Page 717* **2019**, *20* (3), 717.

(85) Amritraj, A.; Wang, Y.; Revett, T. J.; Vergote, D.; Westaway, D.; Kar, S. Role of Cathepsin D in U18666A-Induced Neuronal Cell Death: POTENTIAL IMPLICATION IN NIEMANN-PICK TYPE C DISEASE PATHOGENESIS. *J. Biol. Chem.* **2013**, *288* (5), 3136–3152.

(86) Chung, C.; Puthanveetil, P.; Ory, D. S.; Lieberman, A. P. Genetic and Pharmacological Evidence Implicates Cathepsins in Niemann-Pick C Cerebellar Degeneration. *Hum. Mol. Genet.* **2016**, *25* (7), 1434–1446.

(87) Gabande-Rodriguez, E.; Boya, P.; Labrador, V.; Dotti, C. G.; Ledesma, M. D. High Sphingomyelin Levels Induce Lysosomal Damage and Autophagy Dysfunction in Niemann Pick Disease Type A. *Cell Death Differ.* **2014**, *21* (6), 864–875.

(88) Kosicek, M.; Gudelj, I.; Horvatic, A.; Jovic, T.; Vuckovic, F.; Lauc, G.; Hecimovic, S. N-Glycome of the Lysosomal Glycocalyx Is Altered in Niemann-Pick Type C Disease (NPC) Model Cells. *Mol. Cell. Proteomics* **2018**, *17* (4), 631–642.

(89) Xiong, J.; Zhu, M. X. Regulation of Lysosomal Ion Homeostasis by Channels and Transporters. *Sci. China Life Sci.* **2016**, *59* (8), 777–791.

(90) Abu-Remaileh, M.; Wyant, G. A.; Kim, C.; Laqtom, N. N.; Abbasi, M.; Chan, S. H.; Freinkman, E.; Sabatini, D. M. Lysosomal Metabolomics Reveals V-ATPase- and MTOR-Dependent Regulation of Amino Acid Efflux from Lysosomes. *Science* **2017**, *358* (6364), 807–813.

(91) Soyombo, A. A.; Tjon-Kon-Sang, S.; Rbaibi, Y.; Bashllari, E.; Bisceglia, J.; Muallem, S.; Kiselyov, K. TRP-ML1 Regulates Lysosomal PH and Acidic Lysosomal Lipid Hydrolytic Activity. *J. Biol. Chem.* **2006**, *281* (11), 7294–7301.

(92) Liscum, L. Niemann-Pick Type C Mutations Cause Lipid Traffic Jam. *Traffic (Copenhagen, Denmark)*. John Wiley & Sons, Ltd (10.1111) March 1, 2000, pp 218–225.

(93) Simons, K.; Gruenberg, J. Jamming the Endosomal System: Lipid Rafts and Lysosomal Storage Diseases. *Trends Cell Biol. 10* (11), 459–462.

(94) Duvvuri, M.; Gong, Y.; Chatterji, D.; Krise, J. P. Weak Base Permeability Characteristics Influence the Intracellular Sequestration Site in the Multidrug-Resistant Human Leukemic Cell Line HL-60. *J. Biol. Chem.* **2004**, *279* (31), 32367–32372.

(95) Nietupski, J. B.; Pacheco, J. J.; Chuang, W.-L.; Maratea, K.; Li, L.; Foley, J.; Ashe, K. M.; Cooper, C. G. F.; Aerts, J. M. F. G.; Copeland, D. P.; et al. Iminosugar-Based Inhibitors of Glucosylceramide Synthase Prolong Survival but Paradoxically Increase Brain Glucosylceramide Levels in Niemann–Pick C Mice. *Mol. Genet. Metab.* **2012**, *105* (4), 621–628.

(96) Lee, J.-H.; McBrayer, M. K.; Wolfe, D. M.; Haslett, L. J.; Kumar, A.; Sato, Y.; Lie, P. P. Y.; Mohan, P.; Coffey, E. E.; Kompella, U.; et al. Presenilin 1 Maintains Lysosomal Ca2+ Homeostasis via TRPML1 by Regulating vATPase-Mediated Lysosome Acidification. *Cell Rep.* **2015**, *12* (9), 1430–1444.

(97) Folts, C. J.; Scott-Hewitt, N.; Pröschel, C.; Mayer-Pröschel, M.; Noble, M. Lysosomal Re-Acidification Prevents Lysosphingolipid-Induced Lysosomal Impairment and Cellular Toxicity. *PLOS Biol.* **2016**, *14* (12), e1002583.

(98) Ashe, K. M.; Bangari, D.; Li, L.; Cabrera-Salazar, M. A.; Bercury, S. D.; Nietupski, J. B.; Cooper, C. G. F.; Aerts, J. M. F. G.; Lee, E. R.; Copeland, D. P.; et al. Iminosugar-Based Inhibitors of Glucosylceramide Synthase Increase Brain Glycosphingolipids and Survival in a Mouse Model of Sandhoff Disease. *PLoS One* **2011**, *6* (6), e21758.

(99) Boudewyn, L. C.; Sikora, J.; Kuchar, L.; Ledvinova, J.; Grishchuk, Y.; Wang, S. L.; Dobrenis, K.; Walkley, S. U. N-Butyldeoxynojirimycin Delays Motor Deficits, Cerebellar Microgliosis, and Purkinje Cell Loss in a Mouse Model of Mucolipidosis Type IV. *Neurobiol. Dis.* **2017**, *105*, 257–270.

(100) Lin, H. J.; Herman, P.; Kang, J. S.; Lakowicz, J. R. Fluorescence Lifetime Characterization of Novel Low-pH Probes. *Anal. Biochem.* **2001**, *294* (2), 118–125.

(101) Fraldi, A.; Annunziata, F.; Lombardi, A.; Kaiser, H.-J.; Medina, D. L.; Spampanato, C.; Fedele, A. O.; Polishchuk, R.; Sorrentino, N. C.; Simons, K.; et al. Lysosomal Fusion and SNARE Function Are

Impaired by Cholesterol Accumulation in Lysosomal Storage Disorders. *EMBO J.* **2010**, *29*, 3607–3620.

(102) Mirzaian, M.; Wisse, P.; Ferraz, M. J.; Marques, A. R. A.; Gaspar, P.; Oussoren, S. V.; Kytidou, K.; Codée, J. D. C.; van der Marel, G.; Overkleeft, H. S.; et al. Simultaneous Quantitation of Sphingoid Bases by UPLC-ESI-MS/MS with Identical 13C-Encoded Internal Standards. *Clin. Chim. Acta* **2017**, *466*, 178–184.

(103) Pettersen, E. F.; Goddard, T. D.; Huang, C. C.; Couch, G. S.; Greenblatt, D. M.; Meng, E. C.; Ferrin, T. E. UCSF Chimera - A Visualization System for Exploratory Research and Analysis. *J. Comput. Chem.* **2004**, *25* (13), 1605–1612.

(104) Sievers, F.; Wilm, A.; Dineen, D.; Gibson, T. J.; Karplus, K.; Li, W.; Lopez, R.; McWilliam, H.; Remmert, M.; Söding, J.; et al. Fast, Scalable Generation of High-quality Protein Multiple Sequence Alignments Using Clustal Omega. *Mol. Syst. Biol.* **2011**, *7* (1).

(105) Waterhouse, A. M.; Procter, J. B.; Martin, D. M. A.; Clamp, M.; Barton, G. J. Jalview Version 2—a Multiple Sequence Alignment Editor and Analysis Workbench. *Bioinformatics* **2009**, *25* (9), 1189–1191.

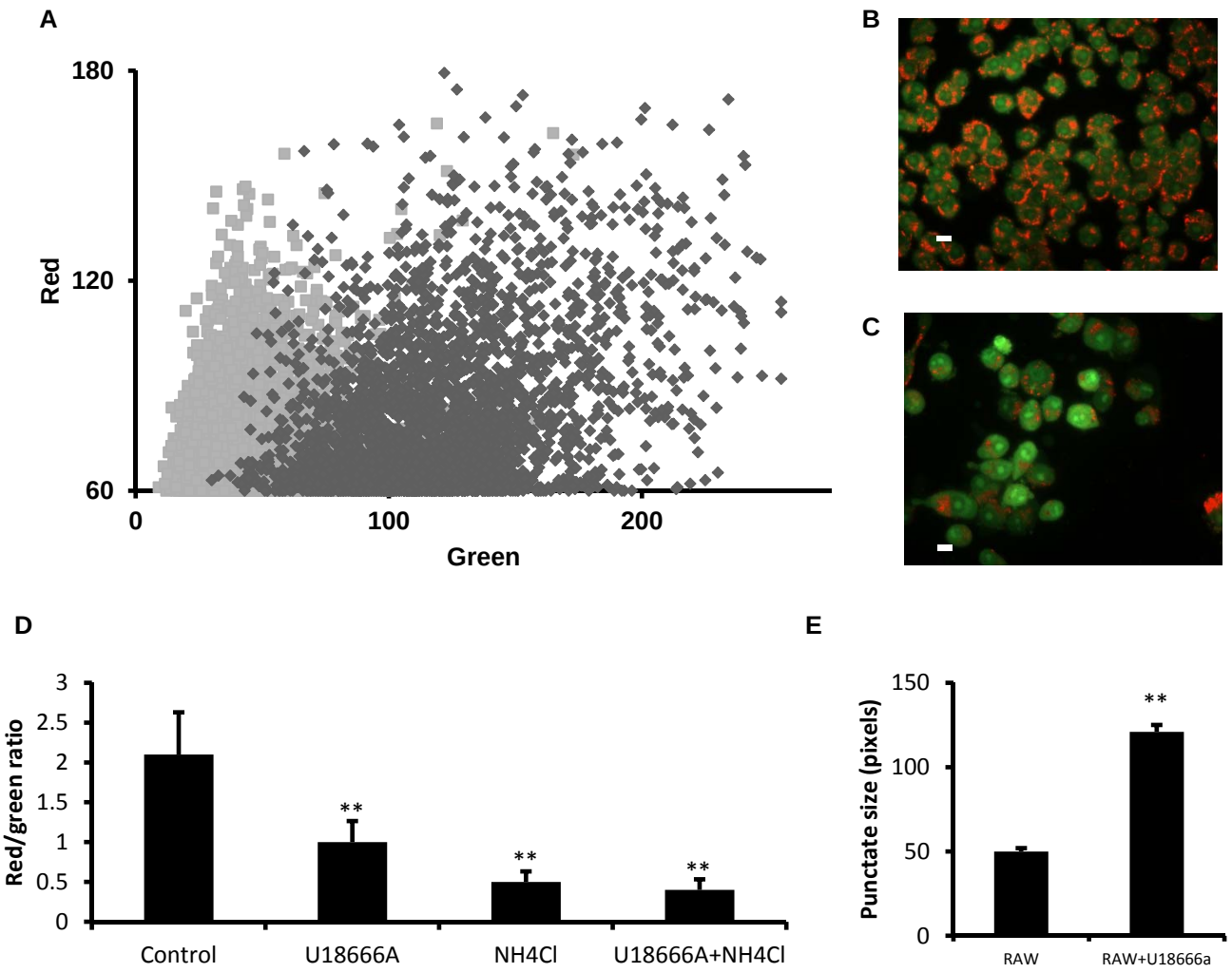


**Figure 1 The size and pH of the endolysosomal compartment increases in RAW cells treated with U18666A A**) Red/Green scattergraph of acridine labelled punctates; untreated (■); U18666A (♦). **B, C**) Representative images of untreated (**B**) RAW cells and cells treated with U18666A (**C**). Scale bars represent 10μm. **D**) Quantitation of red/green ratio in RAW cells in the presence of U18666A, and incubations with cells treated with 10mM $NH_4Cl$. **E**) Quantitation of punctate size in the presence of U18666A. (** $p<0.001$ n=5-10, t-test). Results are presented as mean ± SD (**D**) and mean ± SEM (**E**)

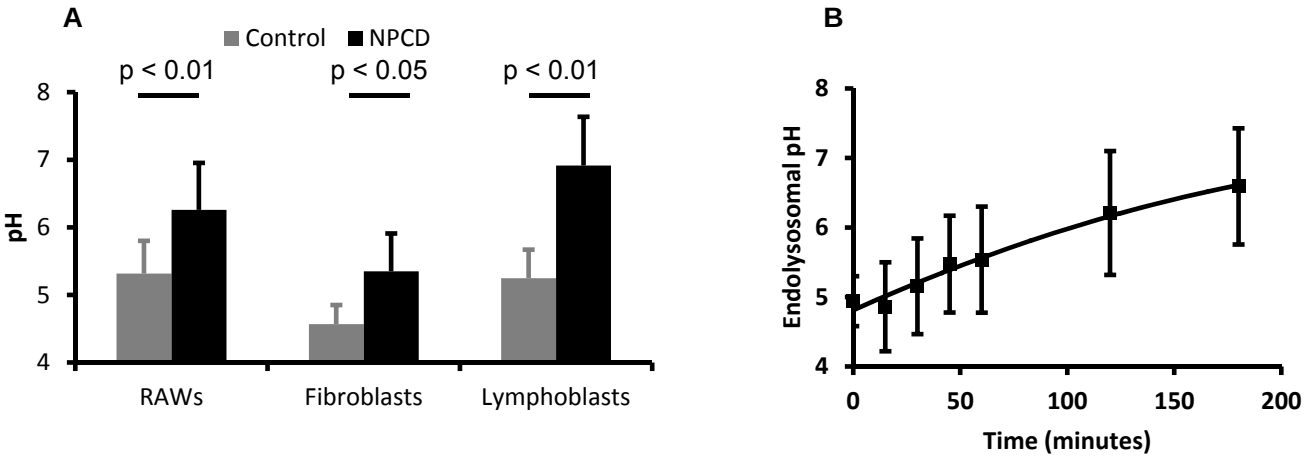


**Figure 2 NPC cell culture models show increased lysosomal pH measured using LysoSensor yellow-blue.** Cells were labelled with 5 μM lysosensor yellow/blue in 1ml RPMI or DMEM (10%FCS) for 5 min at 37˚C. Excess dye was removed by cold PBS. The emission ratio at 451/520 was measured at Ex 320/360nm. RAW cells were treated with 5 μM U18666A for 2.25 hours unless otherwise stated; **A**) Quantitation of lysosomal pH in RAW cells and fibroblasts; n = 4-11, significance measured by t-test and ANOVA) **B**) time course of increased pH in RAW cells treated with U18666A. Significant difference (t-test, $p<0.05$) at 180 minutes but not before. All results are presented as mean ± SD.

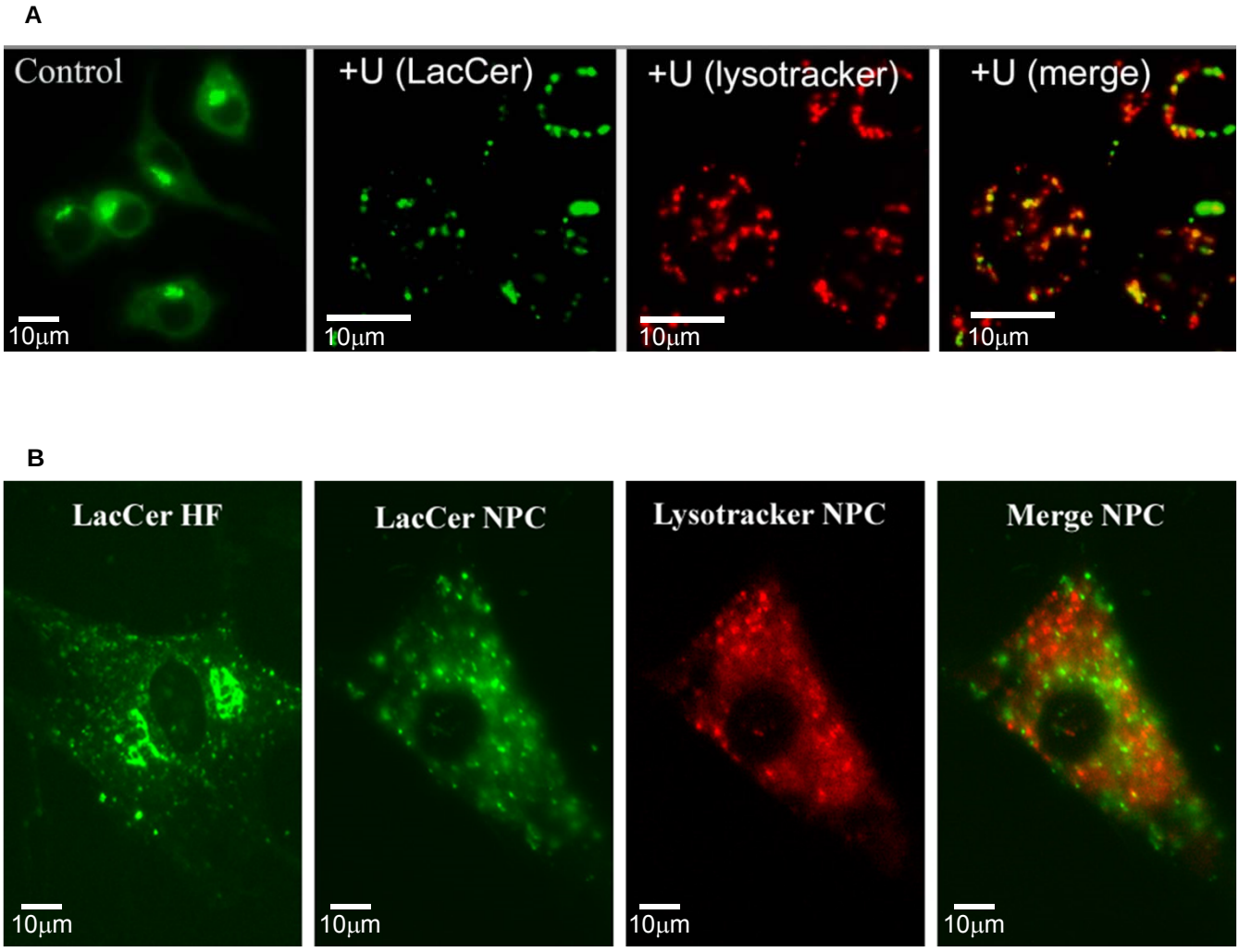


**Figure 3 U18666A gives BODIPY-LacCer trafficking that is disrupted and targets a punctate compartment that partially co-localises with LysoTracker red.** Representative images of RAW macrophages (**A**) and healthy and NPC fibroblasts (**B**) showing the endocytic sorting of BODIPY-LacCer. (Pearson's coefficient RAW 0.51±0.01 n=5; NPCFs 0.17±0.02 n=9). Cells were pulsed for 45mins with 15uM BODIPY-LacCer; RAWs were chased for 60 minutes, fibroblasts were chased for 90 minutes.

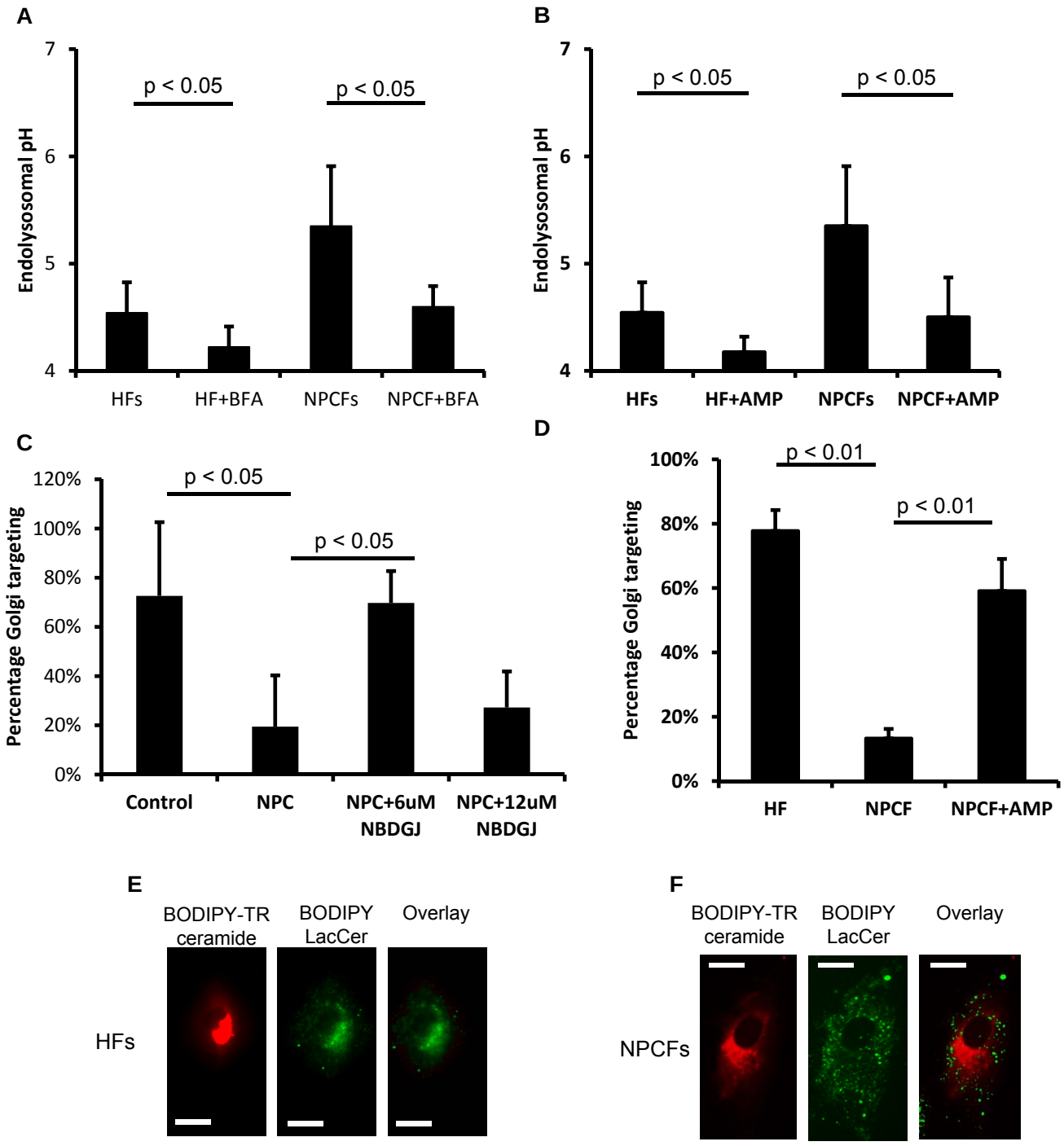


**Figure 4 Repaired endolysosomal pH and Golgi targeting on GBA2 inhibition. A)** Treatment with brefeldin A reduces endolysosomal pH in control and disease fibroblasts. **B**) Endolysosomal pH with and without treatment with AMP-DNJ. Results in **A** and **B** are mean ± SD. **C)** Percentage Golgi targeting in fibroblasts assessed by blind scoring. Percentages are means ± SD from at least 40 cells in at least 2 independent experiments; **D**) Percentage Golgi targeting in fibroblasts with and without treatment with AMP-DNJ as assessed by blind scoring. Percentages are means ± SD from at least 90 cells in at least 2 independent experiments. **E-F)** Representative images of control (**E**) and disease (**F**) cells after pulse-chase treatment with BODIPY-LacCer and BODIPY-TR-ceramide. Cells were pulsed for 45 minutes with 15μM BODIPY-LacCer with 5μM BODIPY-TR-ceramide added for the last 30 minutes. Cells were chased for 90 minutes. Scale bars represent 10 μm. Significance measured by t-test and ANOVA.

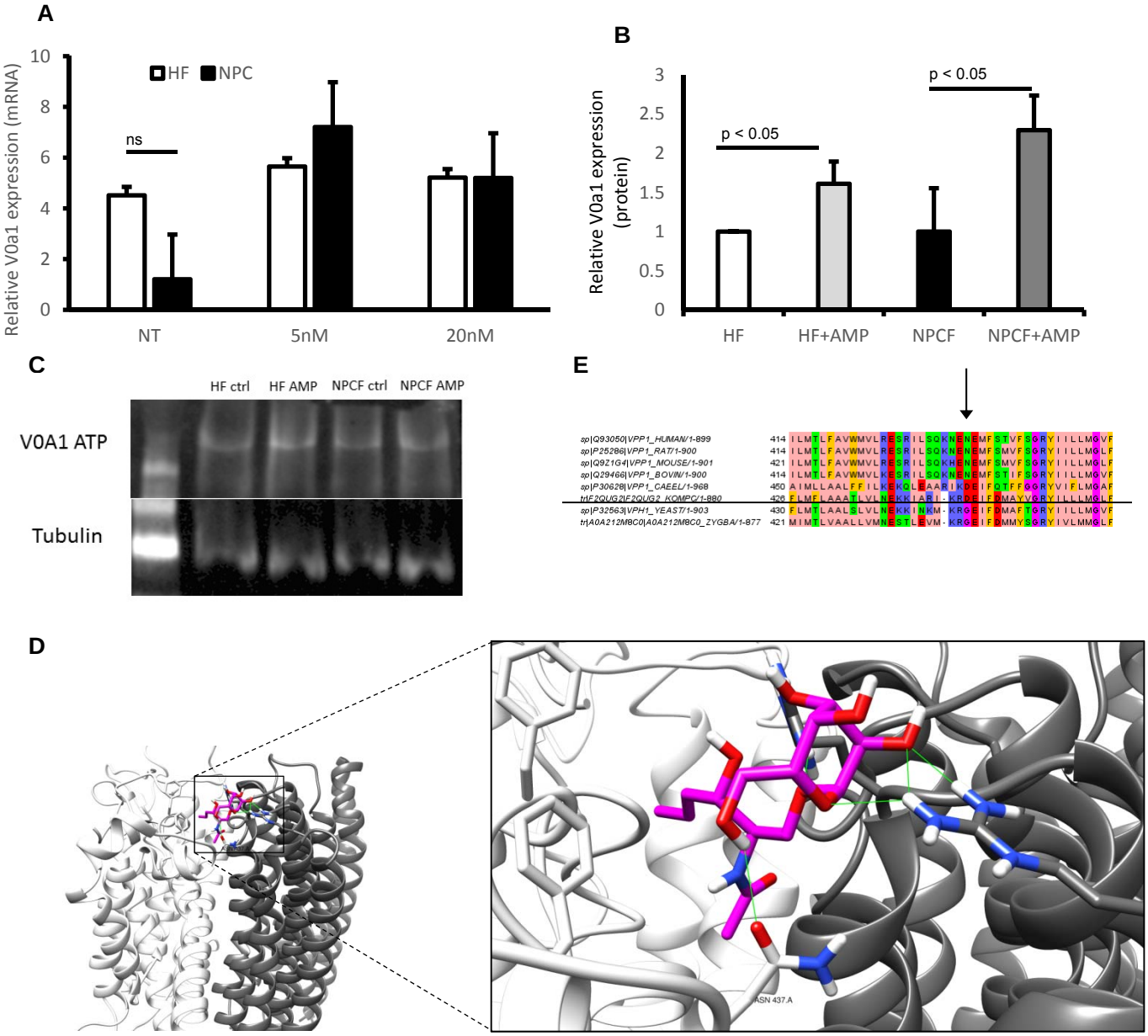


**Figure 5 GlcCer increases expression of vATPase a subunit; potentially critical role of Asn437 A)** In fibroblasts ATP6V0a1 mRNA is unchanged in NPCD, but increased non-significantly by AMP-DNJ. Results are presented as mean ± SD relative to TBP, significance measured by t-test and ANOVA. **B,C)** ATP6V0a1 protein expression is increased by AMP-DNJ in both control and disease fibroblasts consistent with the endolysosomal pH decreases seen with this compound. Results are normalised to untreated healthy cells (n=3). **D)** GlcCer headgroup bridges the vATPase a and c subunits; a subunit reside Asn437 accepts an H-bond (a subunit shown in white, c subunits in grey, GlcCer in magenta, hydrogen bonds as green lines). **E)** Multi-sequence alignment relevant section of the vATPase a subunit from species containing GlcCer (above the line) and in species lacking GlcCer (below the line)

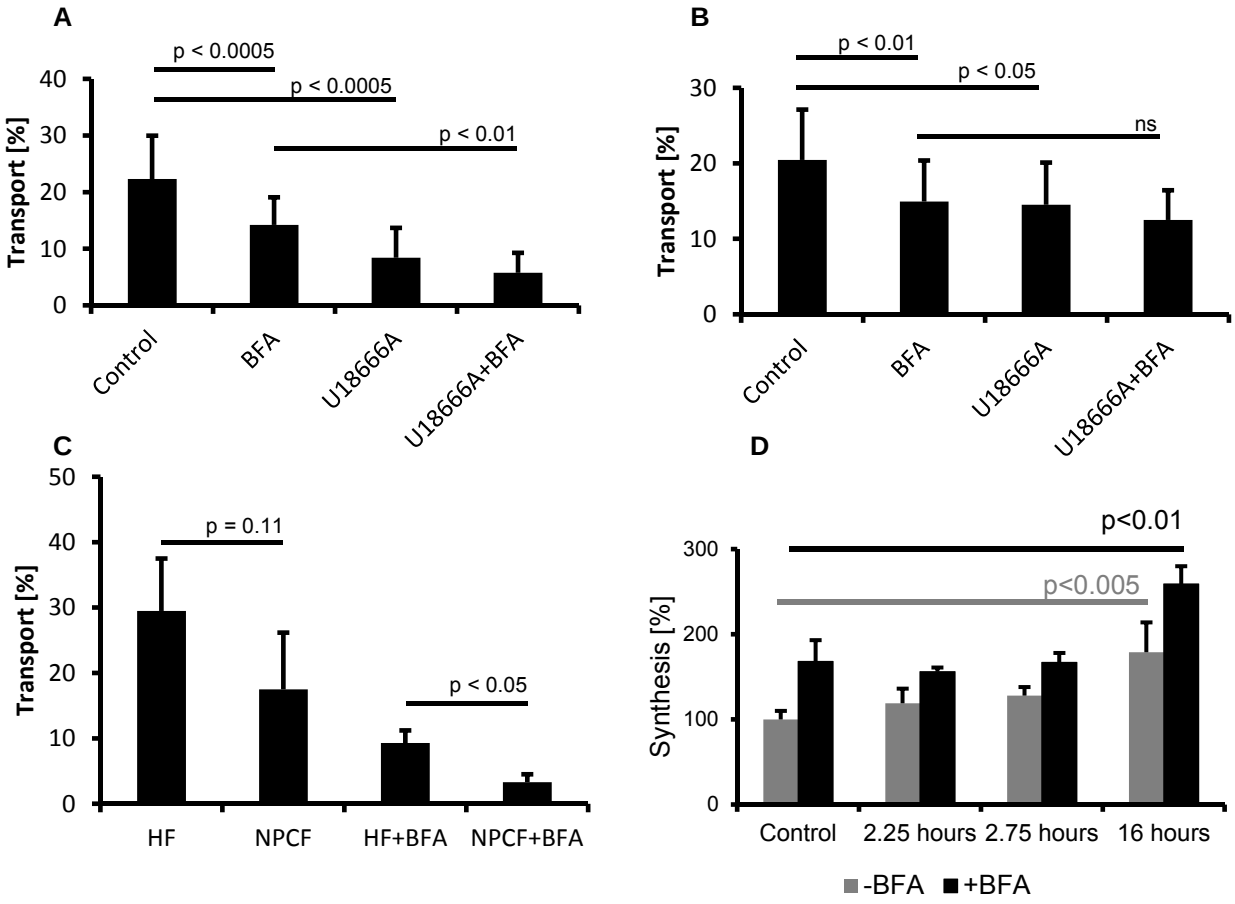


**Figure 6 Transport of newly synthesised GlcCer to the cell surface is reduced in NPCD cell culture models.** The effect of 1µg/ml of brefeldin A (BFA) and 5 µM U18666A on transport of GlcCer (**A**) and GalCer (**B**) by means of the GLTP assay in CHO cells expressed as % transport to the cell surface. **C**) Surface transport of GlcCer in NPC fibroblasts. **D**) U18666A significantly increased amounts of GlcCer at 16 hr in either the presence or absence of BFA; no increases were observed at earlier time points. All samples were pre-incubated ± BFA for 30 mins. Data shown as mean ± SD, significance measured by t-test.

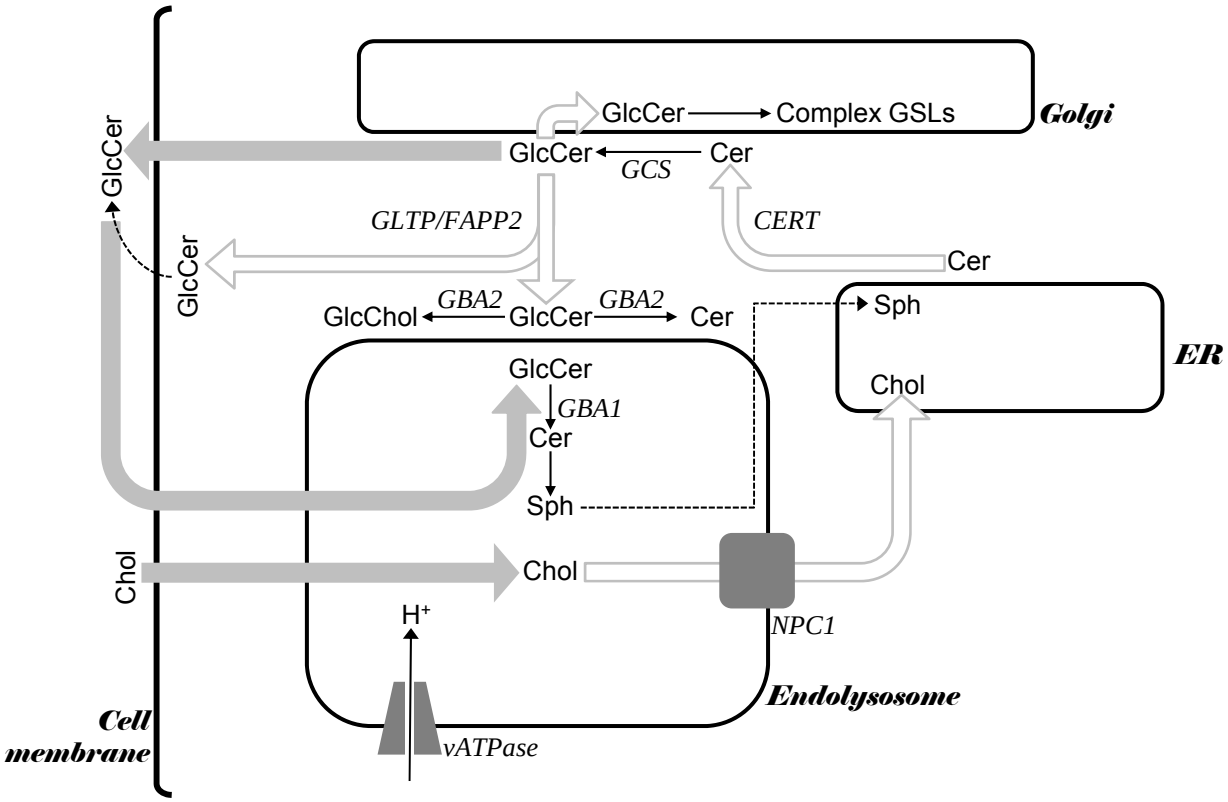


**Figure S1 Selected aspects of lipid metabolism** Black arrows represent metabolic steps; full grey arrows show vesicular transport, hollow grey arrows show non-vesicular transport. Dashed arrows show events which are known to occur but for which a mechanistic understanding is lacking. The transport of GlcCer to the luminal side of the Golgi may not be direct (see refs 57-59)

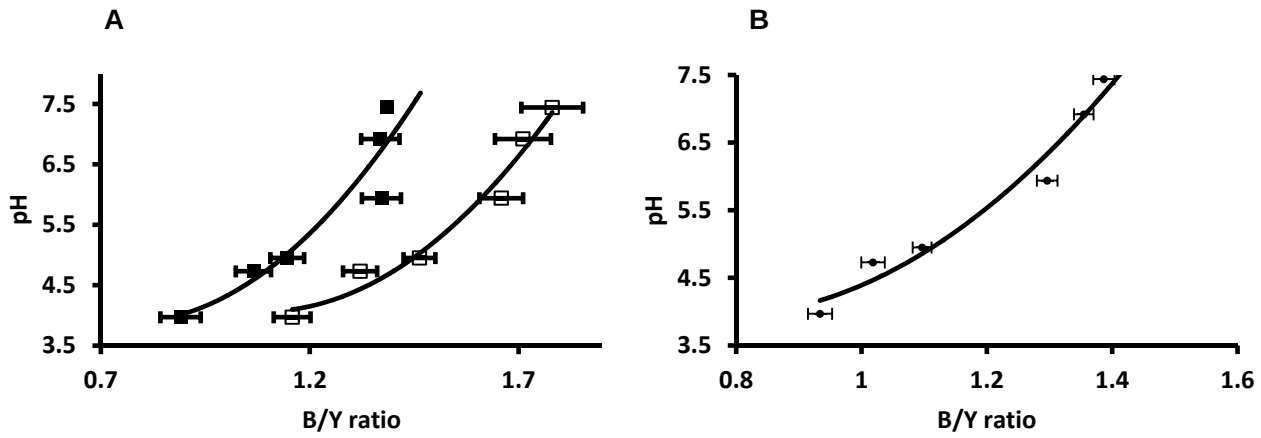


**Figure S2 Correlation curves for pH experiments with LysoSensor yellow/blue A**) Fibroblasts; HFs filled squares, NPCFs empty squares; each data point is the average of readings from independent experiments ± either BFA or AMP-DNJ; non-significant differences (t-test) were observed between datasets (n = 3-6); $r^2$ = 0.89 for HFs, $r^2$ = 0.97 for NPCFs. (**B**) RAWs; each data point is the average of readings from independent experiments ± various drugs; non-significant differences (t-test) were observed between datasets (n=3-11); $r^2$ = 0.97.

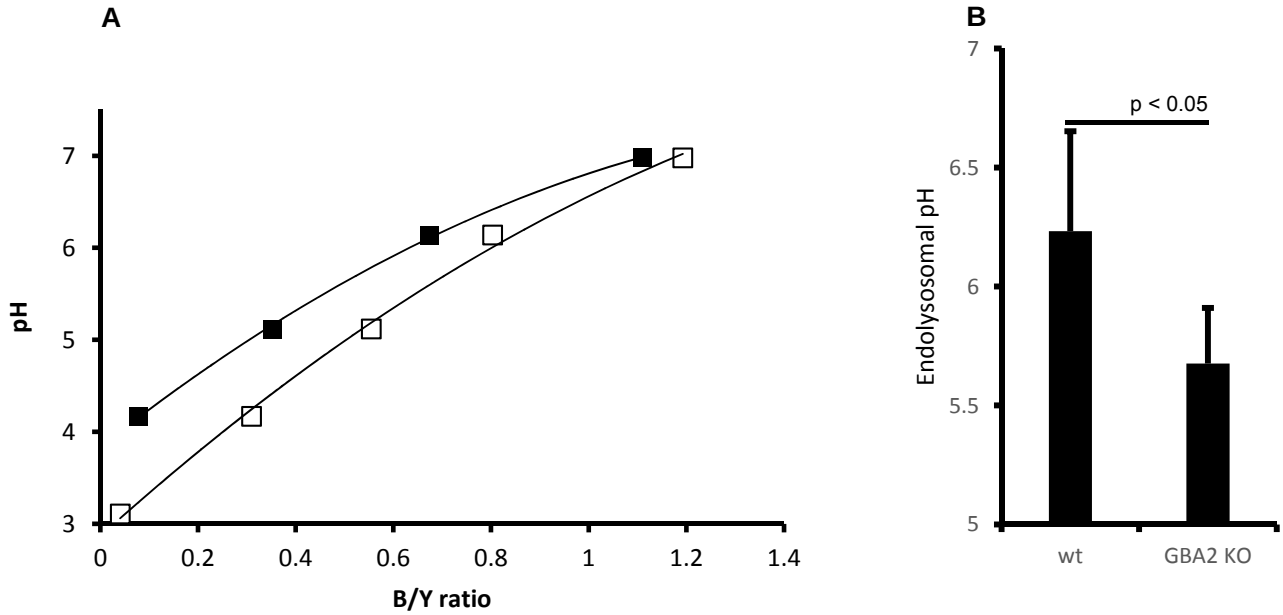


**Figure S3 Measurement of endolysosomal pH in HAP1 cells A)** Sample correlation curves for wt (filled squares) and GBA2 KO (open squares) cells ($r^2$ = 0.999 for wt and 0.997 for GBA2 KO. **B)** Endolysosomal pH in wt and GBA2 KO cells (n=3-4). Data shown as mean ± SD, significance measured by t-test.

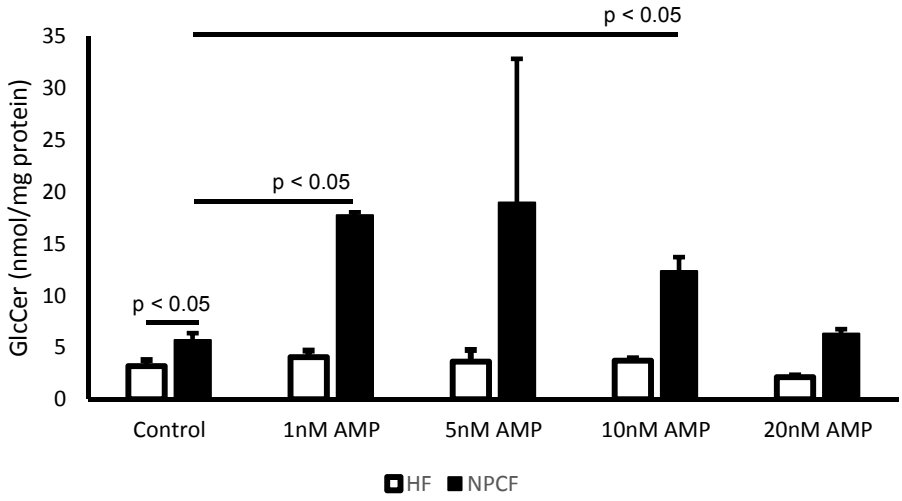


**Figure S4 Variation in GlcCer levels in fibroblasts** The effect on NPCF cells of overnight treatment with 1-20nM AMP-DNJ measured with an HPLC assay; the increase is maximal in the dose range 1-10nM. Data shown as mean ± SD. The large changes seen in Niemann-Pick cells may result from increased GBA2 expression in this disease (see ref 41).

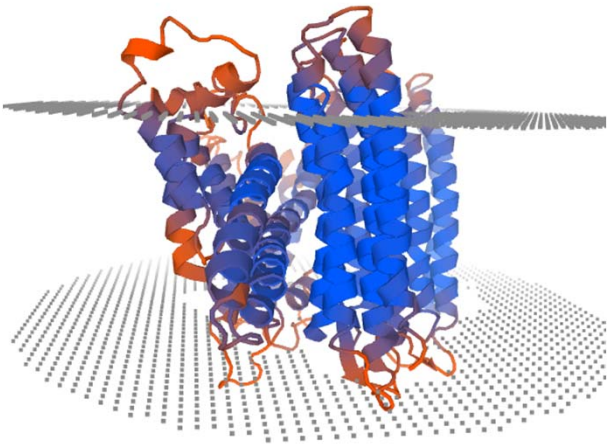

**Figure S5 Approximate position the vATPase model in the membrane** Output from QMEANBrane (swissmodel.expasy.org/qmean/). The model was derived from PDB 5TJ5 as described in the text. This graphic also offer an estimate of model quality ranging from blue (good) to orange (bad)

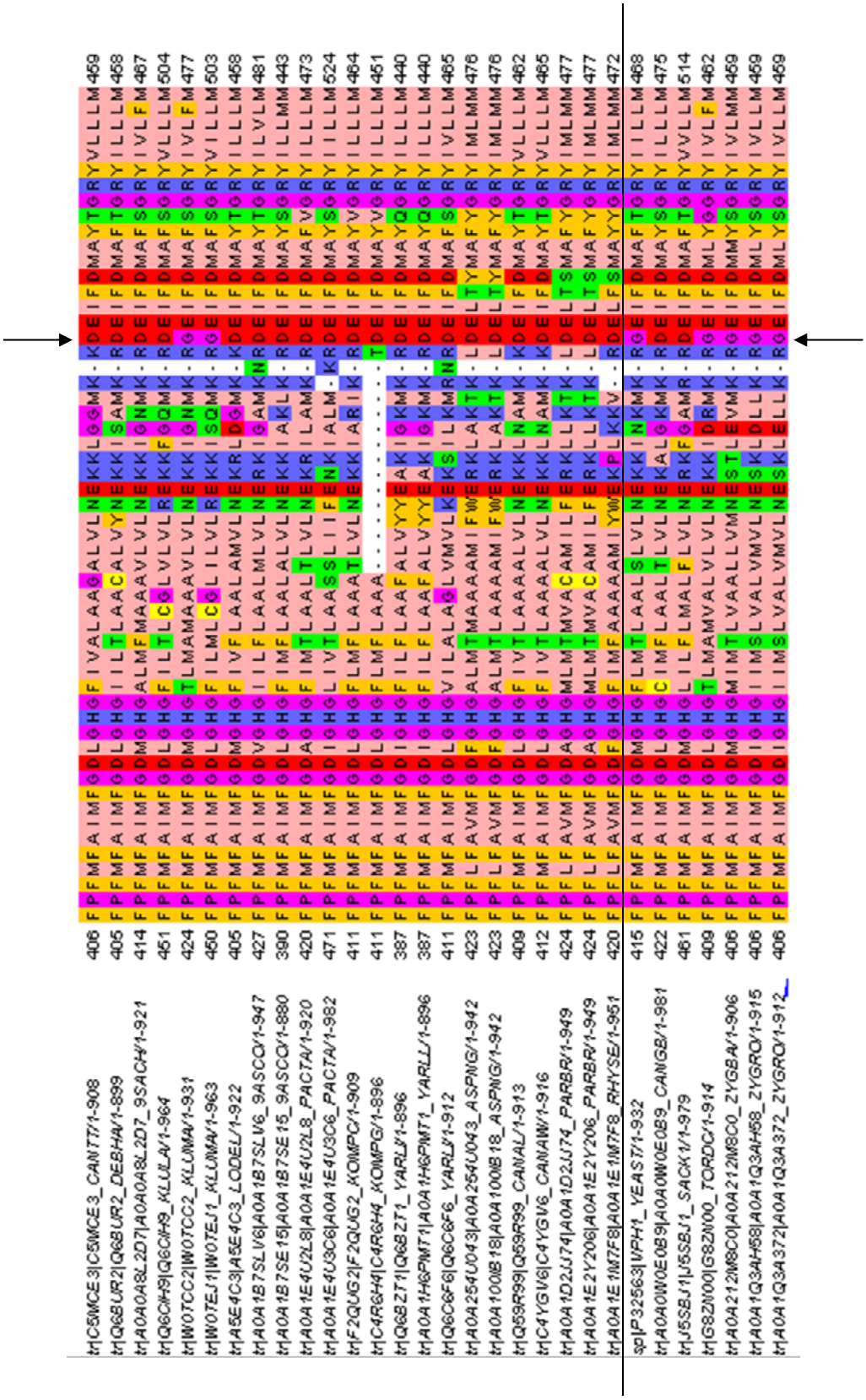

Figure S6 **Multi-sequence alignment of a subunits of yeasts.** Species are divided into those that contain GlcCer (above the line) and those which lack it (below the line) according to Saito et al Appl Microbiol Biotechnol (2006) 71: 515–521 and Warnecke et al Cell Mol Life Sci (2003) 60: 919-41

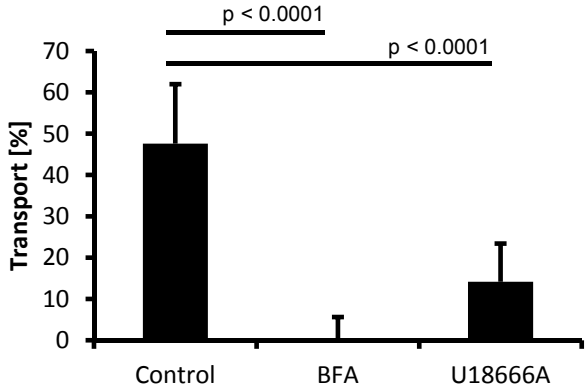


**Figure S7** BFA and U18666A reduce cell surface transport of GM3 using the GLTP assay. Results are presented as mean ± SD.

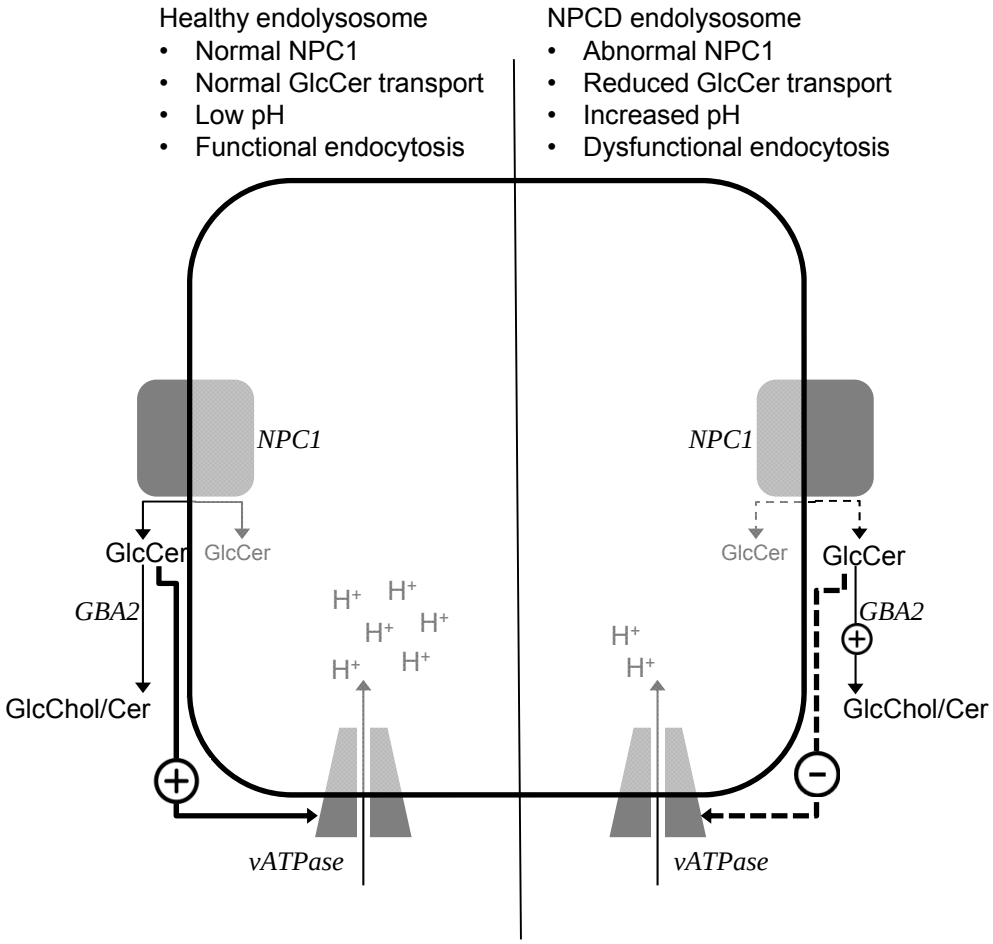


**Figure S8 An endolysosome viewed from the cytosol** Either through increased metabolism or impaired flipping NPCD cells have lower amounts of GlcCer on the cytosolic face of the endolysosome leading to reduced vATPase activation, impaired acidification and dysfunctional endocytosis